DTIC FILE COPY

AUTOMATED IMAGING SYSTEM FOR BRIDGE INSPECTION

Research, Development, and Technology
Turner-Fairbank Highway Research Center
6300 Georgetown Pike
McLean, Virginia 22101-2296

Report No.
FHWA/RD-87/090

AD-A198 844

U.S Department of Transportation
Federal Highway Administration

Final Report
March 1988

DTIC
ELECTE
AUG 2 4 1988
S D
CD

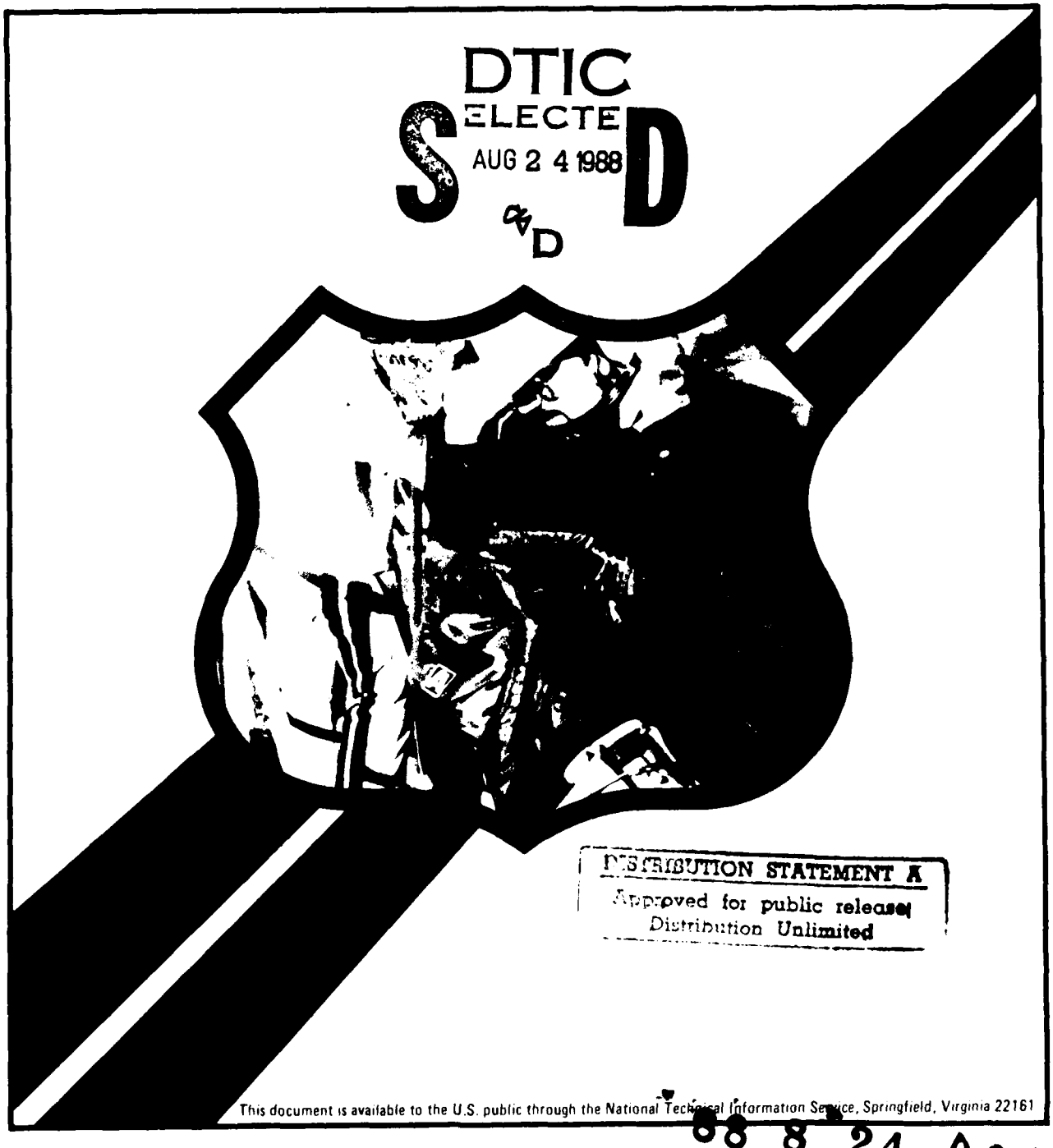

DISTRIBUTION STATEMENT A
Approved for public release
Distribution Unlimited

This document is available to the U.S. public through the National Technical Information Service, Springfield, Virginia 22161

88 8 24 069

Technical Report Documentation Page

1. Report No.	2. Government Accession No.	3. Recipient's Catalog No.
FHWA/RD-87/090		

4. Title and Subtitle	5. Report Date
AUTOMATED IMAGING SYSTEM FOR BRIDGE INSPECTION	March 1988
	6. Performing Organization Code
	8. Performing Organization Report No.
7. Author(s)	
Joseph W. Brophy	
9. Performing Organization Name and Address	10. Work Unit No. (TRAIS)
Sigma Research, Inc. 8710 148th Ave. NE Redmond, WA 98052	FCP 35L2-052
	11. Contract or Grant No.
	DTHF61-83-C-00119
	13. Type of Report and Period Covered
12. Sponsoring Agency Name and Address	Final Report September 1983 to May 1987
Office of Research and Development Federal Highway Administration U. S. Department of Transportation Washington, DC 20590	14. Sponsoring Agency Code

15. Supplementary Notes

Contracting Officer's Technical Representative: Chuck McGogney (HNR-10)

16. Abstract

This report describes the design, operation, and capabilities of the ultrasonic imaging system developed for FHWA. The system uses computerized data acquisition and a lightweight scanner to obtain color-coded images of defects in metal bridge components. Several types of images are obtained, including holographic reconstruction of defects. Defect size, location, and type can be obtained from the images.

This volume is the second in the series. The first volume is:

Executive Summary, Report No. FHWA/RD-87/089.
(This report will not be formally published, but will be available from the National Technical Information Service only.)

17. Key Words	18. Distribution Statement
Ultrasonic, test, imaging, holography, quality assurance, welds, defects, nondestructive evaluation, NDE	No restriction. This document is available to the public through the National Technical Information Service, Springfield, VA 22161

19. Security Classif. (of this report)	20. Security Classif. (of this page)	21. No. of Pages	22. Price
Unclassified	Unclassified	75	

Form DOT F 1700.7 (8-72) Reproduction of completed page authorized

Automated Imaging System for Bridge Inspection

Table of Contents

Page

INTRODUCTION..... 1

BACKGROUND.....2

PHASE I REVIEW - ULTRASONIC METHODOLOGY.....4

PHASE II REVIEW - SYSTEM DESIGN, ASSEMBLY, TEST.....5

Overview..... 5
Hardware Development.....5
Software Development.....11
Scanner Technology.....19
Testing.....21

PHASE III REVIEW - PROTOTYPE DEVELOPMENT, FIELD TESTING.....26

Field System Development.....26
Field Trials.....27
Conclusions of Field Trials.....35

TEST RESULTS ON FLAWS.....37

Phase II Results.....37
Destructive Test Comparisons.....49
Phase III Results.....49

CONCLUSIONS.....58

RECOMMENDATIONS.....60

APPENDIX A - WORK BREAKDOWN STRUCTURE.....63

APPENDIX B - ADDITIONAL COMPONENT BLOCK DRAWINGS.....64

Accession For
NTIS GRA&I
DTIC TAB
Unannounced
Justification
By
Distribution /
Availability Codes
Dist | Avail and/or Special
A-1

LIST OF FIGURES

Figure		Page
1	Automated imaging system for bridge inspection. (a) Uphole system, (b) downhole system	6
2	Bridge inspection system block diagram	7
3	Acoustic mainframe block diagram	9
4	Software hierarchy	12
5	FHWADAQ menu options	13
6	MANPLOT menu options	15
7	Data display menu	16
8	Imaging formats for a defect in the Oregon Graduate Center test sample DF-2. (a) Amplitude, (b) TOF plot, (c) TOF profile	17
9	Image processing options	18
10	Hand scanner	22
11	I-90 bridge between Bellevue and Mercer Island, Washington under construction	28
12	I-90 bridge box girder entry hatch and interior of a box girder	29
13	Inspection in the box girder. (a) Operator using the hand scanner to inspect near a web to girder wall fillet weld, (b) inspectors observing the ultrasonic A-scan signal on the downhole portable monitor	30
14	Uphole system. (a) Control van and communications cable, and (b) operator at the uphole system control console	31

LIST OF FIGURES (continued)

Figure		Page
15	I-205 West Linn bridge. (a) Bridge, (b) snooper crane with inspection team	32
16	I-205 West Linn bridge. (a) Access to girders, (b) inside box girder	33
17	Inspection of West Linn box girders. (a) Inspection team, (b) scanner over bottom flange weld	34
18	Sketch of Lehigh University test samples (not to scale)	38
19	Images of a crack in the Lehigh University test block. (a) 45 degree beam amplitude C-scan, (b) 45 degree beam holographic reconstruction, (c) 60 degree holographic reconstruction	40
20	Planned weld-defect configuration in the Oregon Graduate Center test samples DF-1 and DF-2	41
21	Planned weld-defect configuration in the Oregon Graduate Center test samples DF-3 and DF-4	42
22	Defect in sample DF-4 from the Oregon Graduate Center. Data taken at 45 degrees, 2.25 MHz with a scan size of 7.7 by 3.8 inches. (a) Amplitude C-scan plot with zoomed image, (b) TOF profile	44
23	Amplitude C-scan plots of three defects in test block DF-1. Images obtained using 45 degree beam, 2.25 MHz	46
24	TOF images of the defect in figure 23c	47
25	Defect in test sample DF-2. (a) Amplitude C-scan (3.2-by 2.9-inch scan aperture, 45 degree, 2.25 MHz), (b) TOF profile	48

LIST OF FIGURES (continued)

Figure		Page
26	I-205 West Linn Bridge flange weld locations	50
27	Image of a defect in flange weld A1B4 using a 45 degree, 2.25-MHz beam. Amplitude C-scan using a 25% threshold	51
28	Image of a defect in a flange weld A3B1 using a 45 degree, 2.25-MHz beam. Amplitude C-scan using a 25% threshold	51
29	Map of approximate scan locations in box girder A-weld A1B1	52
30	Image of defect A1B1-A. Amplitude C-scan using a 15% threshold. Scan aperture is 5.73 by 2.25 inches, 5 MHz, straight beam	53
31	Image of defect A1B1-B. Amplitude C-scan using a 15% threshold. Scan aperture is 9.7 by 5.0 inches, 5 MHz, straight beam	54
32	Image of defect A1B1-1. Amplitude C-scan using a 15% threshold. Scan aperture is 4.79 by 4.19 inches, 5-MHz, straight beam	55
33	Image of defect A1B1-2. 5-MHz, straight beam with a scan aperture of 3.68 inches. (a) Amplitude C-scan plot at 15% threshold, (b) holographic result (left: cosine raw data, right: holographic reconstruction magnitude)	56
34	Signal processor module block diagram	65
35	Console junction box block diagram. (All back panel connections go to the communication bundle except the "gated burst" which comes from the signal processor module and the "scanner position out" which goes to the IBM AT serial port.)	66
36	IBM AT card slot assignment diagram	67
37	Belt pack block diagram	68
38	Hand scanner control board block diagram	69

LIST OF TABLES

Table		Page
1	Features of hand scanner	20
2	Phase II laboratory test blocks	23
3	Defect formation for Oregon Graduate Center test blocks	43
4	West Linn Bridge inspection results	57
5	Recommendations for the Automated Imaging System for bridge inspection	61

INTRODUCTION

The goal of this research project was to develop an ultrasonic nondestructive evaluation system that would be capable of field inspection of highway bridges and provide high resolution images of defects. The system would scan and record the data on-site using a lightweight, portable unit with enough flexibility to allow ease of access to truss members, inside box girders, and other typically difficult to reach bridge members. The processing of recorded data would also be on-site by a central processor unit that would be contained in a transportable unit. The transportable unit would contain the necessary power and communication to operate the entire system on a bridge. Data would be stored in digital form to permit further processing at a central location.

The program was divided into three phases. Phase I was to review literature and select the optimum ultrasonic inspection technique for development into the portable automated system. Phase II was the design, assembly, and testing of a laboratory version of such a system. Phase III was the design, assembly, and field testing of a field deployable version of the system. Appendix A contains the work breakdown structure used for this three-phase program.

The program has resulted in a significant accomplishment by developing an automated imaging system that meets the intent of the program. The automated imaging system consists of two major portions and a number of subsystems. The two major portions are the uphole computer data acquisition and analysis system, and the downhole hand-scanner system. The uphole system consists of a computer system with digitizer, graphics display, data analysis software and disk storage, and an ultrasonic mainframe system for ultrasonic transmission/reception and signal processing. The downhole system consists of the special hand-scanner unit, transducer and preamp, as well as a video display link to the uphole data acquisition. A 500-foot communications bundle between the two systems contains power, ultrasonic pulse, ultrasonic signal, video signal, and audio communication. Two operators, one uphole and one downhole operate the system together. They are in communication by audio headsets. This system has been tested and shown to be versatile in data acquisition and data analysis modes. The following report discusses the design and testing of the system.

BACKGROUND

The inspection of highway bridges for defects has consisted predominantly of visual inspection for cracking and corrosion damage. In regions of high stress however, defects that are not visible to the eye may be of safety concern. In these instances ultrasonic inspection offers the inspector the best technique for defect detection. Ultrasound has the advantage of being able to travel large distances in typical bridge structural steels; the technique can be applied in the field with minimal equipment or danger to the public; and it is sensitive to small discontinuities. Interpretation of the signal from a detected discontinuity may reveal a defect that must be watched for future growth or must be repaired.

The most common mode of application of ultrasonics is the A-scan, flaw detection mode. In this case the ultrasonic beam is input to the object using a spike pulse to the transducer. The pulse travels in the part being examined and is reflected from features and discontinuities. The signals that return to the transducer are displayed on an oscilloscope as a waveform trace. The time and amplitude of the return signal are indicative of the location and size of the potential defect. Typically, inspectors move the transducer while observing the waveform on the oscilloscope. In so doing they use their intuitive powers to assess the location and size of defects in the structure. The inspector will also use a test block of structural steel that contains known reflectors such as drill holes to serve as a reference criteria for assessing the size of a defect.

This traditional ultrasonic inspection process contains a number of drawbacks. First, it relies substantially on the skill of the inspector to manipulate the transducer properly, observe changes in the waveform signal, and assess the potential size of the defect. The size will be determined by the area over which the inspector observes the response and the amplitude of response. In the former, because the operator freely moves the transducer, the accuracy of the area determination is limited. In the later, the amplitude response alone from defects is known to be poorly correlated to actual defect size. Because this data is observed on the oscilloscope, it is not recorded for post test evaluation. All decisions on the raw data must be made at the time that it is being observed. The record of the data and defect is the hand-written field report of the inspector. This presents serious problems for repeat testing to follow crack growth. The records

are subjective in nature and do not conform to standards for meaningful repeat examinations if close monitoring of a defect is necessary.

The need for better technology is obvious and well recognized by the FHWA, funding this program to develop an automated imaging system is proof of that need. Defect imaging is the best method to obtain repeatable, measurable data. The equipment to develop this capability must be designed for rugged field environment use. Traditional laboratory systems using motor-driven mechanical scanners and water tanks would not apply to the problem. However, a portable hand-scanning device which provides positional information from a hand-scanned area of interest on a bridge structure would serve as a key element in a total system. With this positional information, the ultrasonic signal can be processed and digitized for analysis by a computer. Such a system would provide record keeping of detected defects. Data processing could provide defect characterization, particularly sizing information. And, the standardized data acquisition would allow for repeat measurement of defects that is essential for crack growth observation.

PHASE I REVIEW
ULTRASONIC METHODOLOGY

The Phase I activity included a survey of ultrasonic flaw detection, data recording,and flaw imaging. From this survey four techniques were selected as candidates for development under this program. The four techniques were confined-beam, synthetic aperture focusing technique (SAFT), holography, and stepped-frequency imaging (SFI). These techniques are discussed in the Phase I report, "Automated Imaging System for Bridge Inspection, Phase I," Report No. DTFH61-83-R-00127.

The conclusion of the Phase I review was that coherent holography should form the basis for the imaging system. This conclusion resulted in component selection for data acquisition, storage and processing that could provide the necessary accuracy. By achieving these goals the system also serves as a high-resolution, confined-beam imaging system. The confined beam technique can be used for most applications that do not require the higher resolution of coherent holography reconstruction. However, when it is necessary to obtain the highest resolution flaw imaging then the system can utilize its holographic reconstruction algorithms. Data processing in this case is more time-consuming than the confined-beam approach. Essentially the confined-beam data can be useful in near real-time while the holographic processing is a post data acquisition analysis package.

PHASE II REVIEW
SYSTEM DESIGN, ASSEMBLY, TEST

Overview

The Phase II activity involved the design, assembly and testing of a laboratory version of the automated imaging system for bridge inspection. A number of components needed to be tested to develop a useful state-of-the-art system. Two essential developments were the signal processing system for acquiring the desired information from the ultrasonic waveform and a scanner device capable of providing position information of the transducer location during field inspection on the bridge structure. Additionally, a computer system was required that could handle the volume of data envisioned and which could process and display the data at an acceptable rate. Other hardware would be required to make these components operate together as a system, such as digitizers, power supplies, signal communication, displays, etc. The Phase II activity defined the requirements for the components to be used in the total system. Prototype equipment was purchased and assembled, and data processing software was developed. Testing was performed on test blocks to verify that the data acquisition and analysis system was useful for detecting and characterizing flaws of interest in bridge structures.

Hardware Development

The hardware developments for the system involved breaking the total system into two major portions: an uphole system and a downhole system. Figure 1a and figure 1b are photographs of the uphole and downhole parts of the system. Figure 2 shows the total system block diagram. The downhole system is shown inside the dotted box. The downhole system contains the hand scanner with a transducer, a belt pack containing a preamplifier and interconnection junctions, a television monitor, and a headset. A 500-foot communications bundle connects the downhole system to the uphole system. The uphole system contains a junction box for communications interface, an ultrasonic mainframe with a special signal processing module, a computer with a digitizer and a color graphics display.

The acoustic mainframe is the heart of any ultrasonic inspection equipment. The unit developed for the automated imaging system uses Metrotek ultrasonic receiver and gate modules

(a)

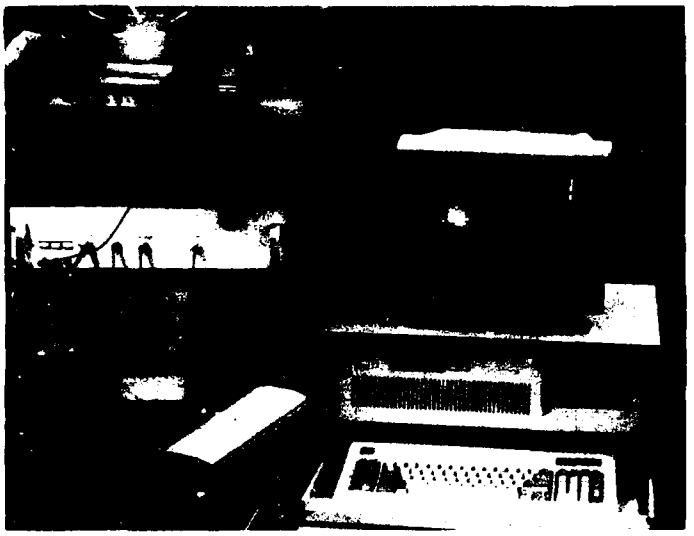

(b)

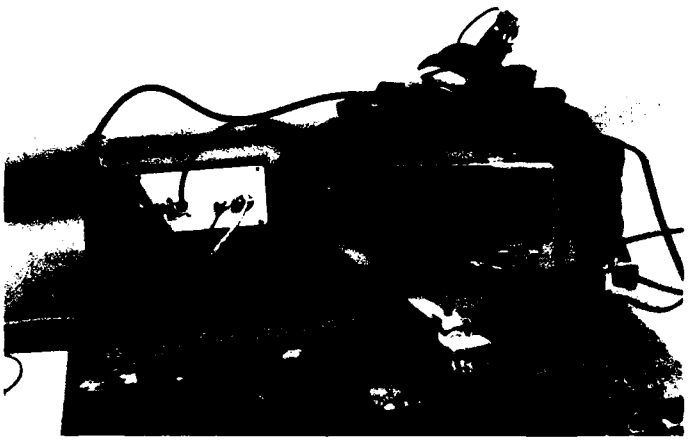

Figure 1. Automated imaging system for bridge inspection. (a) Uphole system; (b) downhole system.

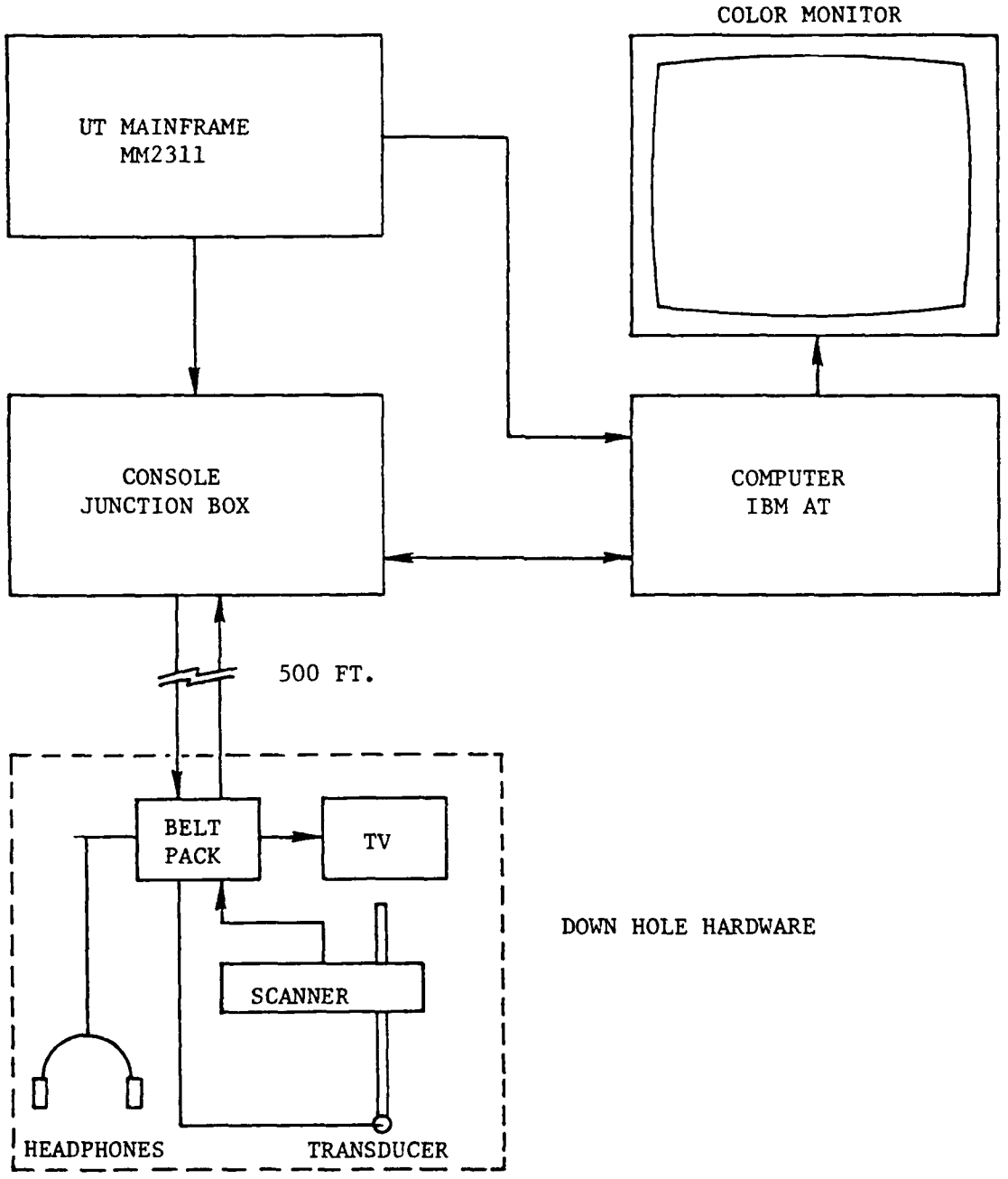

Figure 2. Bridge inspection system block diagram.

in a Tektronix power supply bin. A Tektronix oscilloscope is included in the bin to display the raw waveform and gate signals. A Sigma Research special signal processor module is mounted in the Tektronics supply. Figure 3 is a block diagram of the acoustic mainframe.

The signal processor module is the key element in the design of this acoustic mainframe. The module processes the ultrasonic waveforms to provide the necessary data input to the computer system. The desired data information is the peak amplitude in the gate, the time of flight in the gate to the first signal above a preset threshold (0.25- to 0.5-Volt range) and the holography coefficients. In order to obtain the holography coefficients, the signal processor module provides a gated-tone-burst signal. The module will use this tone burst as a reference signal which it mixes with the return ultrasonic response to create the proper interference information for acoustic holographic data acquisition. The gated burst is output to a power amplifier which transmits the pulse over the 500-foot cable to the transducer. The return echoes from the transducer go to the receiver unit. The gain of the signal level may be adjusted by attenuation settings on the receiver module. The waveform is displayed on the oscilloscope. A gate module is used to select the region of interest in the waveform. The gate may be positioned in size and location along the waveform by adjustments on the gate module. Data will be taken from the gated region by the signal processor module. Four outputs: peak amplitude (amp), time of flight (TOF), holographic sine coefficient (sin), and holographic cosine coefficient (cos) are sent to the digitizer in the computer.

The computer used in the Phase II effort was an Intel 310. This computer uses an Intel 8086 microprocessor with 640k system memory. The operating system was a modified CPM. The use of the Intel computer in Phase II revealed difficiencies in its operation and serviceability. Near the completion of Phase II a failure of the hard disk in the computer resulted in a loss of capability to analyze Phase II data. For the Phase III program it was decided to reconfigure the system with IBM-AT computer using the disc operating system. The IBM-based computer provides a more standardized system for multiple-station implementation and better service support. Unfortunately data taken with Intel 310 system has a unique CPM format and cannot be viewed with the IBM-AT system without significant modification to the data format. The computer includes a digitizer that converts the output voltages for the amplitude, TOF, sin, and cos signals from the signal processor module to digitized values for storage and display.

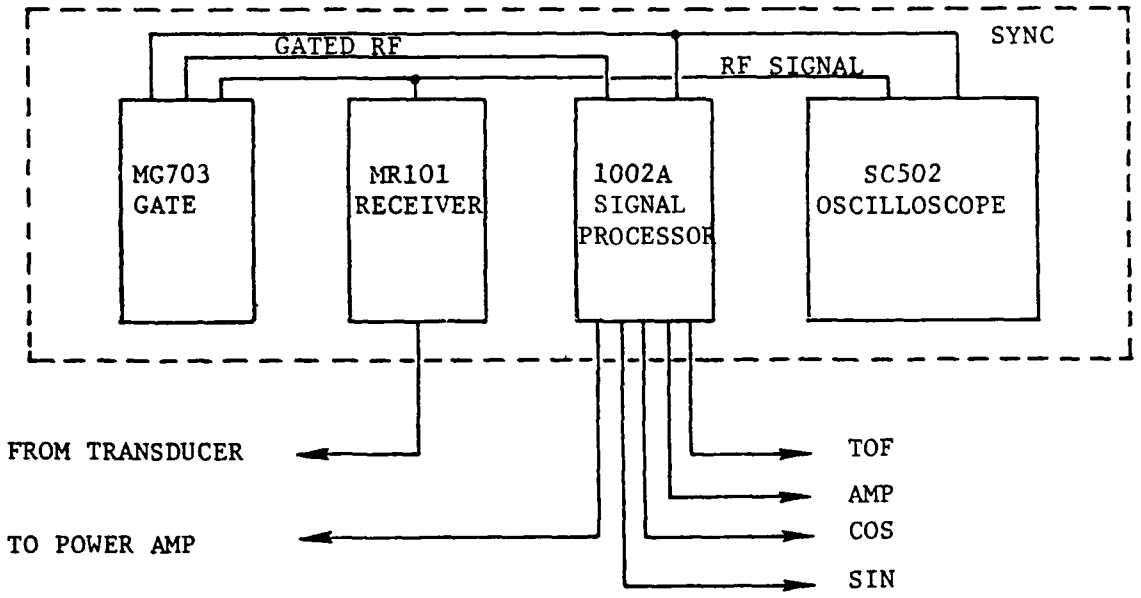

Figure 3. Acoustic mainframe block diagram.

The operation of a field bridge-inspection system requires that the equipment be lightweight and easily transported to the often difficult-to-reach areas to be inspected. The inspector must have his hands free for climbing about the structure but must have enough information available to him to be able to make on-the-spot decisions with regard to the inspection results. This is accomplished by packaging only essential elements in the downhole system and leaving the heavier equipment uphole. The communications to the uphole data acquisition system is through a 500-foot cable bundle. The 500-foot distance is suitable for most all bridge inspections that were considered by expert personnel involved in the program and also allows signals to be transmitted without requiring added amplification. The connections are located in a specially developed belt-pack that the downhole inspector wears on his waist. The beltpack contains a preamplifier to boost the transducer signal before sending it over coax line to the receiver module. The inspector also carries a television monitor. The monitor is in communication with the uphole system where the uphole operator may display either the computer graphics output or the oscilloscope waveform over the video line.

A hand scanner that provides the essential position information and resolution has been developed. This scanner is designed to be lightweight (4 lbs) and rugged for field use, yet inexpensive in case it is dropped or lost during inspection. The scanner has an aperture size of 11 by 7.5 inches. It is a hand scanner because this technique allows the inspector the greatest amount of flexibility. A motorized version was designed, however testing and discussions with bridge inspectors revealed that there are few advantages and considerable drawbacks to a motorized version. Primarily the hand scanning has the greatest versatility for inspection. The inspector mounts the transducer in the scanner and scrubs about the area of interest. Good transducer contact can be maintained in this manner and the inspector is in control of the equipment at all times. The scanner has a resolution of 0.010 inches. Details of the scanner development are in a following section.

Additional diagrams for the equipment developed in the Phase II portion of the program are given in appendix B. The appendix B diagrams include any updates or changes as a result of the Phase III effort.

Software Development

Special software was required for the development of this system. During Phase II much of the software was developed for the Intel 310 computer using the CPM operating system. In Phase III this software was converted to the DOS operating system for the IBM-AT. Figure 4 is the software hierarchy for system. There are three main codes in the software operating system: FHWADAQ, MANPLOT and HOLOIM. The main codes utilize various include-files for data manipulation and display.

The FHWADAQ code is the data acquisition code. Figure 5 lists the menu options available. This code directs the setup of the scanner for data acquisition and displays the resulting data. Prior to performing the hand scanning, the inspector uses 'Initialize Aperture' to set up the scan aperture. This is accomplished by positioning the hand scanner in the upper left portion of the scan aperture and responding to the computer prompts and then moving to the lower right portion and responding to the computer prompts. An important feature of this code is that during data acquisition, the graphics display screen is painted with dots as the inspector scans the transducer about in the hand-scan aperture. By observing the dot pattern the inspector can evaluate how well the data acquisition is progressing and where remaining data must be taken. If the inspector retraces a location the data will be rewritten for that location only if a larger value has been sampled. This feature ensures that if the couplant begins to fail in later stages of scanning the earlier data, which would be superior, is not overwritten. Likewise if the inspector improves the ultrasonic contact during scanning, the better data is recorded. The data acquisition software stores digitized values of amp, TOF, sin and cos signals. These values are stored in respective files of amplitude, TOF and holography data.

The FHWADAQ program has a data header input routine. The header input specifies the parameters used in the data acquisition process. The name used to designate the header is the same as the name that designates the data set. The code allows data to be taken and the header input afterward. Data must be saved to avoid being lost when FHWADAQ is exited, however the code prompts the operator to save the data in the event that it is not saved at the time it is taken. The FHWADAQ code also allows data currently taken to be displayed and processed.

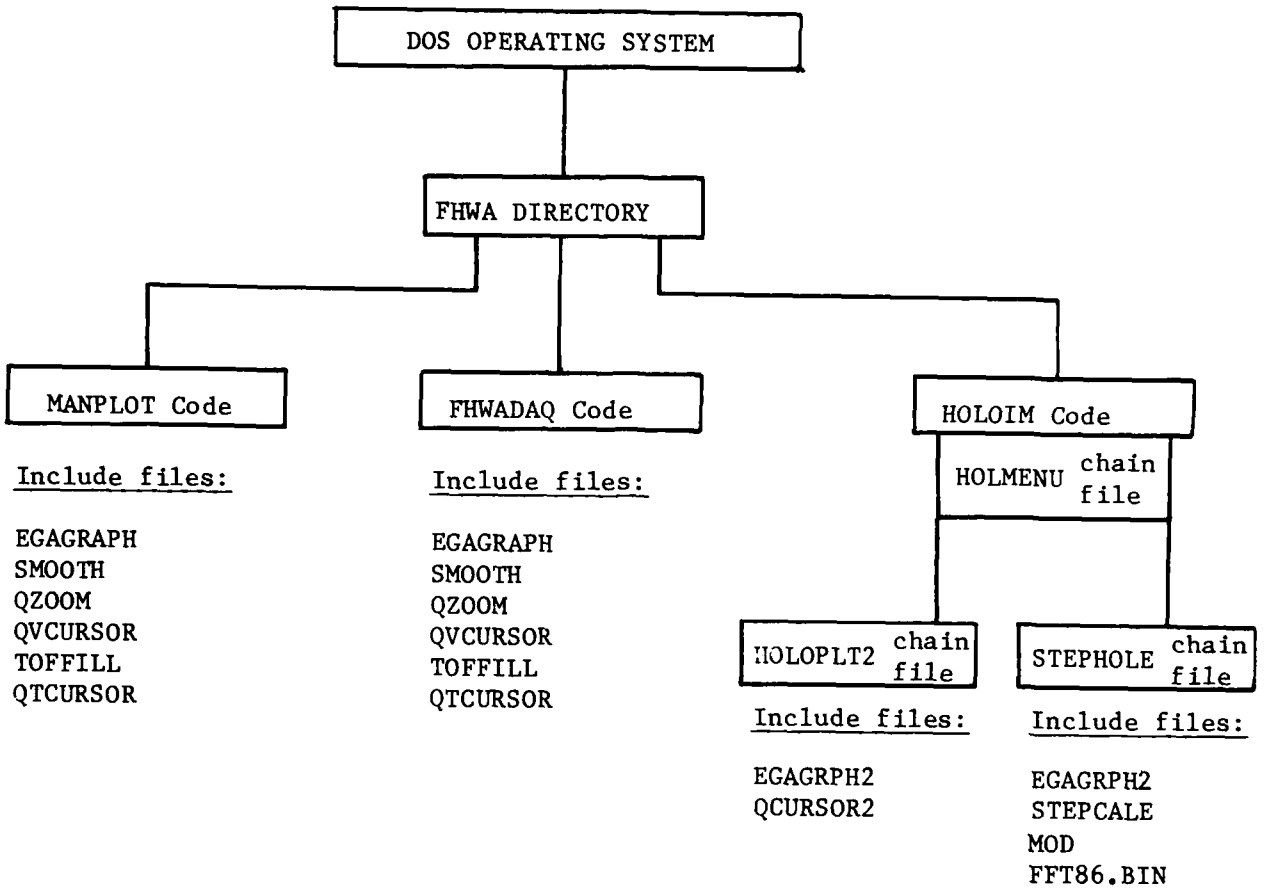

Figure 4. Software hierarchy.

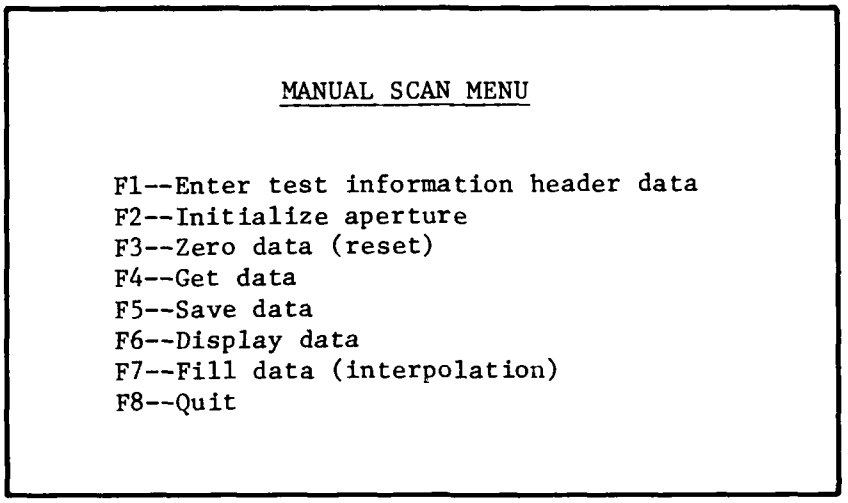

Figure 5. FHWADAQ menu options.

The MANPLOT code takes data that has been previously recorded by the FHWADAQ code and allows it to be post test processed. MANPLOT is used for reviewing old data while FHWADAQ is used for new data. The MANPLOT menu options are shown in figure 6. These options are similar to the FHWADAQ options.

The 'Fill Data (Interpolate)' option is important for data taken with the hand scanner. The hand-scan data sets will have pixels that have true data readings and pixels that have missing data. This routine analyzes the data and fills in missing points using an averaging technique. The averaging scheme uses an inverse square distance weighting to each useful data point surrounding the missing pixel. The routine also includes an evaluation of the quality of the data in terms of the sufficient number of pixels to represent the flaw. This evaluation uses information based on the raw data to interpolated data ratio, the number of empty pixels to pixels that had true data and an evaluation of the magnitude of the signals as a function of distance from the peak signal pixel.

After the data has been interpolated the 'Data Display' option is selected. Figure 7 shows the data display menu. The sin and cos options are not useful displays from this menu because they require a holographic reconstruction prior to display. Their purpose is to verify that adequate data was acquired. The amplitude and time-of-flight displays are very useful. Figure 8 shows the amplitude plot, TOF plot and TOF profile for a real defect data set. In figures 8a and 8b the larger boxed area is the image. The smaller rectangular side boxes are data profiles in the x and y direction. The profiles are displayed for the pixel location on the image of maximum value when the image is first displayed. A cursor is also displayed at this location. The cursor may be moved about the image using the direction keys on the keyboard. The location and pixel value at the cursor is updated as the cursor moves. Figure 9 lists optional data interpretation routines that can be performed from these displays by selection of function keys. F1 and F2 allow distances on the image to be measured. By selecting F1, moving the cursor and selecting F2 a distance value between the cursor locations when the F1 and F2 were selected will be displayed. F3 and F4 display the profiles at the current cursor location by either overlaying or updating the display. F7 and F8 are zoom routines. The zoom routines enlarge the area center about the cursor position by the zoom factor specified. The pixel zoom performs pixel replication which does not improve the resolution. The smooth zoom uses an interpolation of the data in the zoom process which improves the

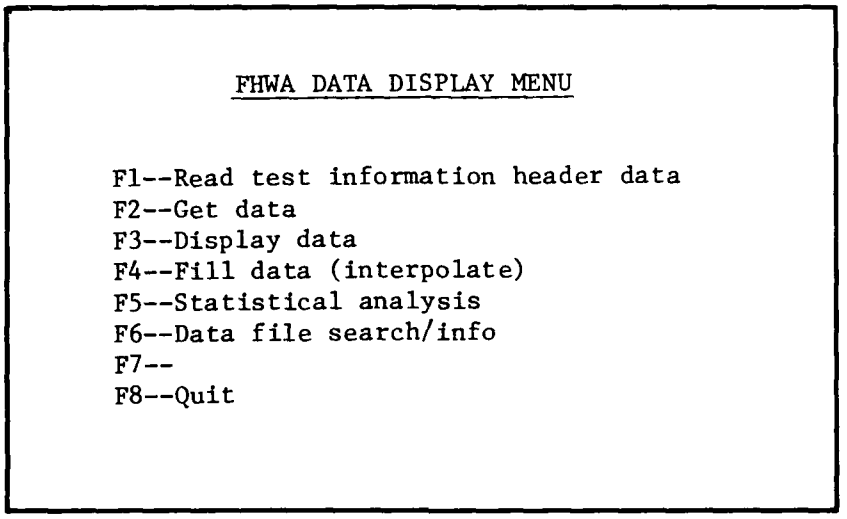

Figure 6. MANPLOT menu options.

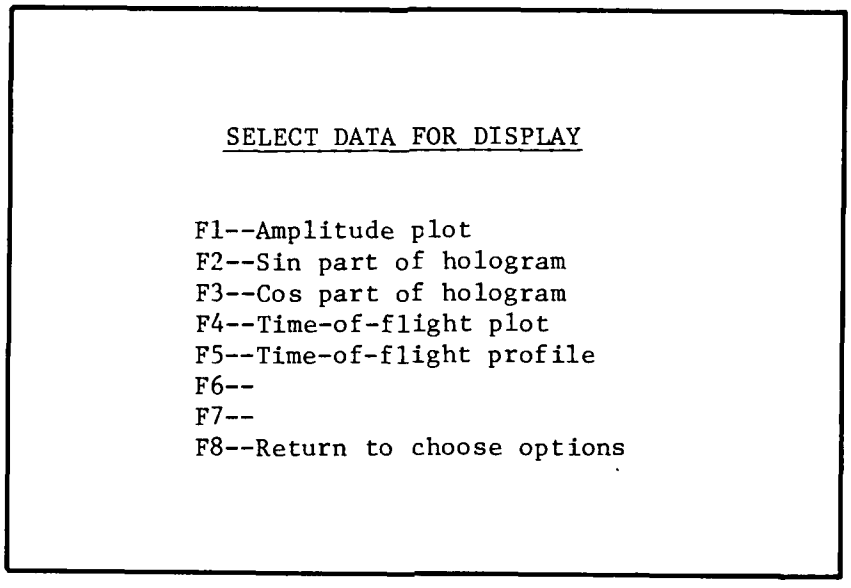

Figure 7. Data display menu.

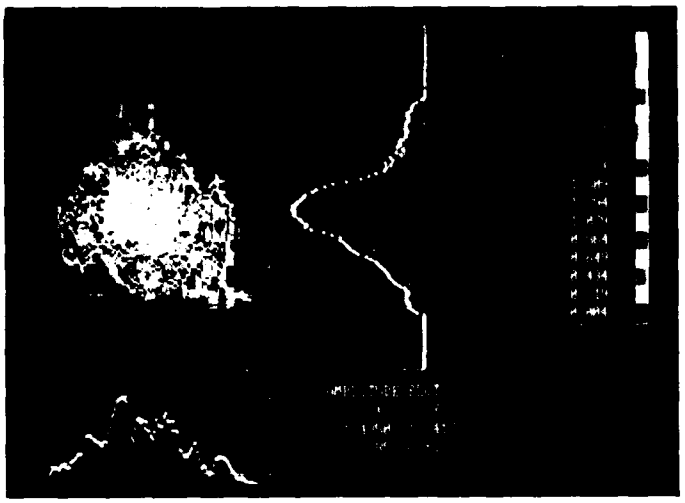

(a)

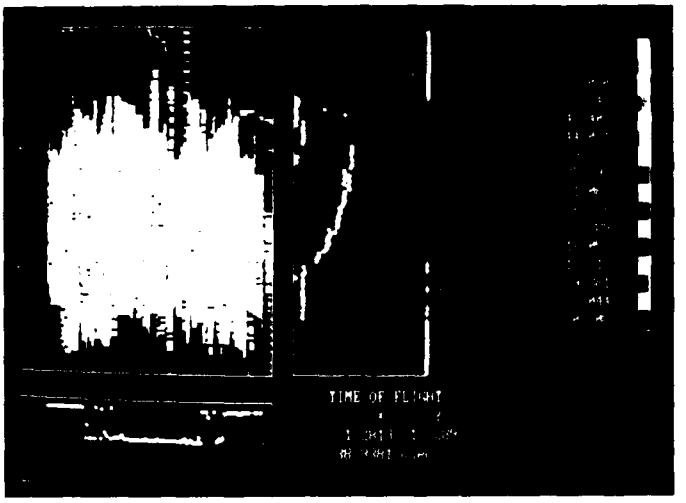

(b)

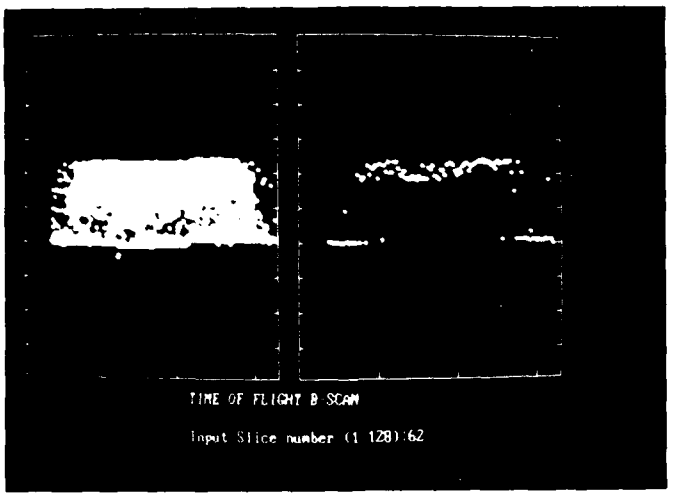

(c)

Figure 8. Imaging formats for a defect in the Oregon Graduate Center test sample DF-2. (a) Amplitude; (b) TOF plot; (c) TOF profile. Note that reproduction of the color images from the computer graphics to black and white photographs causes a distorted gray scale image.

F1--Start position for distance measurement in the xy plot
F2--Stop position for distance measurement in the xy plot
F3--Overlay profile data at the current cursor position
F4--Erase old profiles and plot profiles at the cursor
F5--No action
F6--Erase Profile plots
F7--Pixel replication zoom
F8--Smooth zoom
F9--ADR (Adjacent data recognition) function

Figure 9. Image processing options.

resolution in the image. The interpolation window size depends on the zoom size. F9 is an adjacent data recognition routine which smooths the data by averaging a pixel with its surrounding eight neighbors.

The usefulness of the displays depends on the information desired. The amplitude display is useful for measuring the rough size of the defect in its plotted dimensions. The size measurements are easy to perform by positioning the cursor and taking distance readings. The TOF displays are useful for determining through wall dimensions of a defect based on the time response for the front surface of the object, back surface of the object and the defect. Time measurements may be made by movement of the cursor. The defect size obtained from the conventional amplitude display will most likely over estimate the size of the object for a given threshold criterion. Only if the object size exceeds a prescribed safety value in the amplitude plot does the higher resolving power of the holographic reconstruction method need to be used.

The HOLOIM code is used for processing the holographic data. The first step is to interpolate the holographic coefficient data. This is not done by the 'Fill Data' routine in MANPLOT or FHWADAQ because a more sophisticated interpolation is required which is both time-consuming and requires a new data file to be created. Interpolation is performed by a holography plotting code (HOLOPLT2). After interpolation the new interpolated data file is used in the holographic reconstruction analysis. The reconstruction code (STEPHOLE) displays a menu of the data parameters, allowing the angle and velocity values to be changed if desired. The raw interpolated data is plotted. The operator may then select reconstruction of the backprojected image. A depth (Z value) for reconstruction must be input. The data will be processed and an image created. If a reconstruction at a second depth is desired the analysis program is restarted and a new depth value for reconstruction input. A 'B-scan' holography option is available for a given Y location in the XY raw data plot. A range of Z (depth) values are used in the backprojection calculation. This result is useful for determining the correct focus depth if it is not known.

Scanner Technology

The development of the hand-scanner technology is one of the most significant items developed in this program. Table 1 lists

Table 1

Features of hand scanner

Lightweight	-	4 lbs.
Accurate	-	0.010 inches
Rugged	-	Can withstand reasonable shocks and field environments.
Fast	-	Provides correct position information at scan rates to 20 inches/second.
Inexpensive	-	Less than $3,000
Versatile	-	Variable-mounting configuration. Can be used with various transducers. Variable-aperture size to 11x17 inches. Transducer can be manipulated on arm for uneven surfaces.

the major features that make the technology so important. Prior to this development there was no suitable system for field inspection of structures such as bridges because all other scanners require significant mechanical setups, precision arrangements, or particular orientations. The economic value of such systems also prohibited their routine use in dangerous environments.

Figure 10 shows the hand scanner. It consists of a base and an arm. The transducer mounts to the arm. The transducer mount is jointed for scanning on contours. The mount uses V blocks to grip a 0.375-inch diameter rod. In most cases the transducer base, or shoe in the case of angle beams, will require a modification which attaches a vertical rod to the transducer unit. The rod should be aligned with center of the transducer beam at its exit point from an angle-beam shoe. The scanner arm and base both contain linear optical slide encoders. The arm is easy to move in both X and Y directions. While the optical encoders should be kept clean, they function with a minimum of care even in dirty environments. A special microcomputer board, located in the uphole console junction box, is the position controller which relays the information to the data acquisition computer. The scanner itself can be moved at rates up to 20 inches per second without losing position information. The system data acquisition rate however is determined by the uphole computer speed which results in an overall rate of about 4 to 5 inches per second. Scanning at rates faster than 4 to 5 inches per second results in missed data points in the graphics displays. These positions may be easily retraced for complete filling.

High accuracy in the scanner is essential for holographic images. The scanner is accurate to 0.010 inches. The maximum scanner aperture size depends on the size of the base and arm. Sizes up to 11 by 17 inches have been used, however, the Phase III field trials resulted in a compromise size of 11 by 7.5 inches as being the most useful.

Testing

Phase II testing was performed on laboratory test blocks. Table 2 lists the test blocks that were available from various agencies. Not all of the test blocks contained flaws. The Wisconsin DOT and the General Dynamics test blocks were used to test ultrasonic beam behavior in materials that had very different grain sizes in the weld zone. The Wisconsin test blocks were

Figure 10. Hand scanner.

Table 2

Phase II laboratory test blocks

Source	Quantity	Description
Wisconsin Dept. of Transportation Madison, WI	3 blocks	Electroslag weldments in A-441 steel. Blocks were 6 inches x 36 inches with variable thickness. Block 1 - 1.5 inch Block 2 - 1.5-2-inch transition Block 3 - 3-3.5-inch transition The blocks contained no real defects only 3/32 inch side drilled holes.
General Dynamics Groton, CT	1 test plate	HY80 GMAW welded plate 24 inches x 24 inches x 1.5 inches marine structural material
Lehigh University Bethlehem, PA	2 blocks	Cover plate tc I-beam flange welds. Four cover plate welds per block. Flange thickness of 2 inches, cover plate thickness of 1 inch. Overlap of 6 inches. Welds were fatigued to grow cracks.
Oregon Graduate Center Portland, OR	4 blocks	Welded A-36 steel specimens typically 24 inches x 24 inches. Thickness of 3 inches in first block and 2 inches in remaining three blocks. Numerous inclusions, cracks, and defects in welds.

welded using an electroslag technique and had coarse grain size in the weld zone, whereas the General Dynamic test block used a different welding technique that produced a very fine grain size in the weld zone. In addition, some of the Wisconsin test blocks had thickness transitions that were useful for testing the attachment of the scanner mechanism and the ability to acquire useful data from configurations that have significant thickness variations. The Lehigh University test blocks contained fatigue cracks and the Oregon Graduate Center test blocks had a wide variety of defects in the weld zone. Results of the testing measurements are given in the 'Test Results' section of this final report.

The testing phase determined that the acoustical system developed in the program would be effective for inspection in the materials of interest. As discussed earlier in this report, the acoustic mainframe uses a tone-burst output. This creates a narrow-band signal. Most conventional ultrasonic systems use a spike pulse, broad-band signal. In some materials the broad-band signal can have advantages for overcoming frequency-dependent attenuation and for providing good time resolution. The narrow-band signal of the automated imaging system has been found to operate well in the materials tested at a frequency of 2.25 MHz. The tone-burst length when amplitude and TOF information is desired is usually kept short (1 microsecond). For holographic imaging, it is better to use longer tone-bursts of four to six microseconds.

The ultrasonic measurements used both straight beams (zero degrees) and angle beams for inspection. The test-block studies found that angle-beam inspection is the best method for obtaining return signals from cracks. The use of angle beams requires a plastic shoe to refract the sound at the part/material interface. The TOF data display in MANPLOT and FHWADAQ does not correct for the delay time in the shoe. The operator must consider this in interpreting angle-beam data. In fact, images created by angle-beam measurements do require greater interpretation skills than the straight-beam images particularly for surface breaking cracks. The advantage of the automated imaging system is that it allows consistent and repeatable images to be created with the angle-beam inspection. Nevertheless, the inspector must understand the geometry to assess the defect extent.

Imaging in the test specimens of Phase II also found that the confined-beam (amp and TOF) image displays provided nearly as good a resolution as holography. This is to be expected for the

thicknesses of the specimens encountered in bridge structure test samples. Acoustic holography is best on thick structures where broad-beam coverage can be generated. The transducer selection for the optimum confined beam imaging is not the optimum for holographic imaging. The confined-beam technique is best with a transducer having very little beam spread while holography requires a wide ultrasonic beam to provide maximum coverage in the part. It is this wide coverage that allows the coherent imaging of holography to be effective. Thus, two scans over a region of interest may be necessary if the best images for both confined beam (amp and TOF display) and holographic reconstruction are desired. In most cases the confined beam image is sufficient for satisfactory flaw characterization for defects with short sound paths.

The separation of flaw detection and flaw characterization is not clearly defined for bridge inspection. Economic use of an inspection system dictates that the least amount of time needed to verify the presence or absence of defects be used. The procedures and parameters that enhance the ultrasonic detection of a defect's presence are seldom appropriate for the best characterization. By necessity the bridge inspection system is a compromise between the two types of desired information. It provides better record keeping, a series of post analysis options and maintains a reasonable level of detection flexibility. The alternative would be to use different types of ultrasonic instrumentation and procedures for either detection or characterization and would require much more time and effort to effectively deploy on a bridge.

PHASE III REVIEW
PROTOTYPE DEVELOPMENT, FIELD TESTING

Field System Development

During Phase III a field operational prototype system for automated imaging has been developed. As discussed in the Phase II review, some modifications were made to the laboratory system for more effective field operations. The computer was changed to an IBM-AT with 640k memory and the software was changed to the DOS operating system. The software is also written primarily in TURBO Pascal (trademark of Borland International) version 3.0 and must be compiled with a 8087 numeric coprocessor version of the TURBO Pascal compiler. The computer has a 1.2 Mbyte high-density floppy drive, a 360k floppy drive and a 20 MByte hard disk. For field use, the hard disk may not boot the system when it is cold. A startup disk in the high-density floppy drive is used as a more reliable device for field work.

The uphole system is packaged for transportation in a van. The acoustic mainframe, power amplifier and console junction box are mounted in a portable rack cabinet. The computer is mounted in a lockable transport box on a computer stand. The color graphics display monitor is attached to the computer transport box. Two television cameras are used with the uphole system to view the oscilloscope and graphics monitor for transmission to the downhole operator. A power conditioning unit is part of the uphole system which must be used between the system and the field power generator.

The downhole components are all contained in padded carrying pouches. The headset voice communication between the uphole and downhole operators requires no power so that it is not subject to interruption or failure due to loss of power or battery life. The 500-foot cable bundle which connects the uphole and downhole systems is mounted on an easily handled cable reel and transport frame.

Figure 1 showed the uphole and downhole portions of the prototype field system. The setup and operation of the field system is described in the operation and maintenance manual. A videotape has also been produced which shows how the system is interconnected and operated.

Field Trials

Field testing of the system has been performed at two locations in the Pacific Northwest. The first trials were on the I-90 bridge between Bellevue and Mercer Island, Washington. Two box girders were inspected at this location. The second location was the I-205 West Linn bridge outside of Portland, Oregon.

The I-90 bridge structure is shown in figure 11. The main support structure consists of six steel box girders for each traffic direction. The entry hatch and inside structure of the girders are shown in figure 12. In figure 13, an operator is using the hand scanner to inspect a web to stiffener fillet weld. The "A-scan" data is being observed on the portable video monitor. Figure 14a shows the control van near the bridge. The 500-foot communication cable bundle is shown on its deployment spool and transport stand near the van. Figure 14b shows an operator at the uphole system control console. Both the uphole and downhole operators are wearing headsets for communication. The uphole system shown in this deployment trial differs from the final Phase III prototype shown in figure 1. This trial in early July of 1986 used the Intel 310 computer. No defects were expected or found during this test.

The I-205 West Linn bridge structure is shown in figure 15. The design uses box girders similar to the I-90 bridge but on a larger scale. A key concern in this structure are welds in the bottom flange of the box girders. Figure 15b shows a snooper crane lowering an inspector with the automated imaging system over the side of the bridge to inspect these welds from the outside. Figure 16 shows access to the inside of the girders from the roadway. In figure 16a, the workers are running the communication cable from the uphole system control van into the manhole access to the inside of the girder. Figure 16b shows the inside of the girder with the communication cable lying on the girder bottom flange. Figure 17a shows workers in the girder. Figure 17b shows the hand scanner ready to inspect a bottom flange weld.

The West Linn bridge has four main girders (A,B,C and D). A previous inspection report noted defects at locations in girders A and D. During this field trial reinspections were performed at several locations in girder A using both outside and inside positioning of the automated imaging system on the box girder. Results of the measurements are presented in the 'Test Results' section of this report.

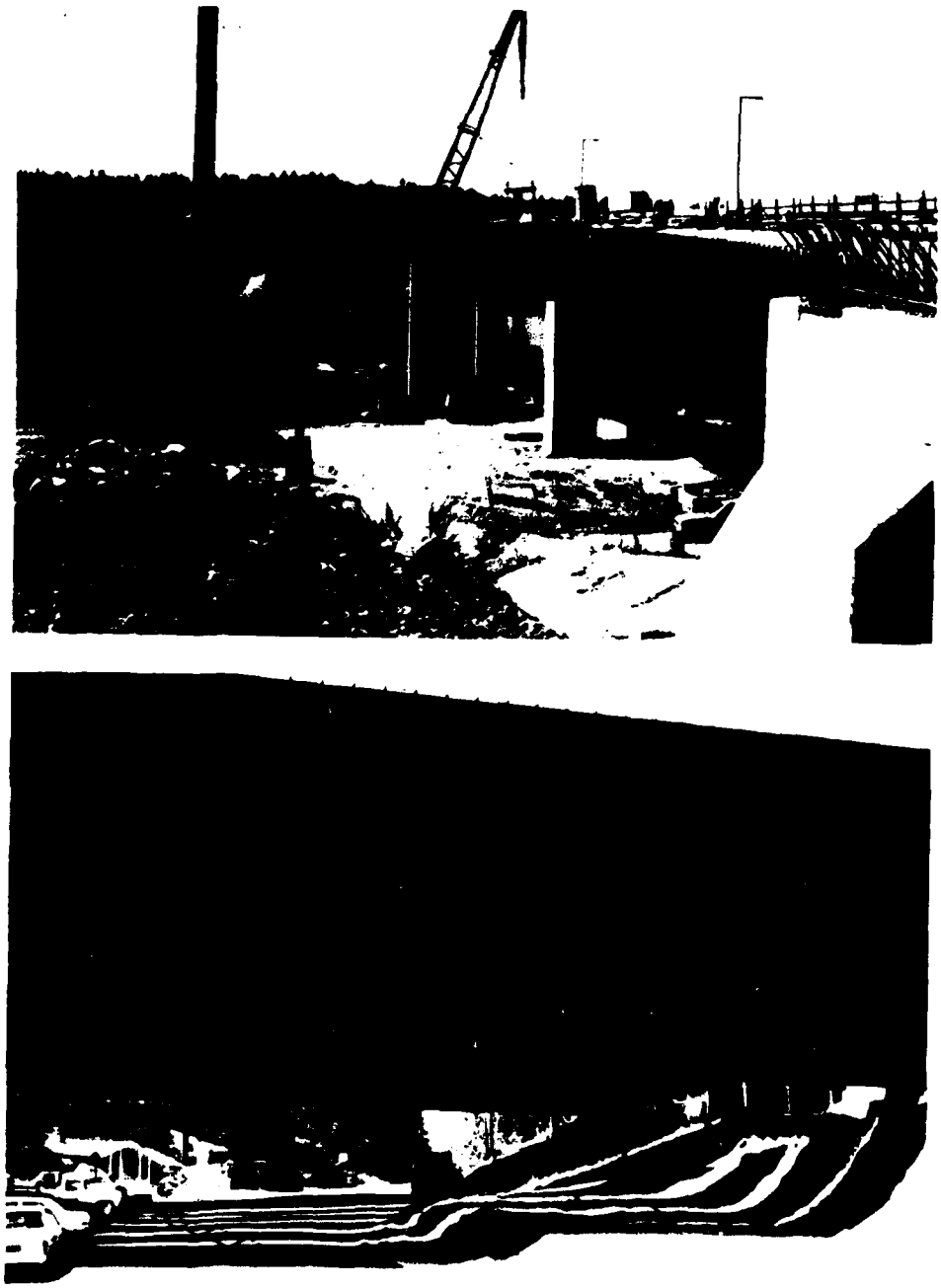

Figure 11. I-90 bridge between Bellevue and Mercer Island, Washington under construction.

Figure 12. I-90 bridge box girder entry hatch and interior of a box girder.

(a)

(b)

Figure 13. Inspection in the box girder. (a) Operator using the hand scanner to inspect near a web to girder wall fillet weld; (b) inspectors observing the ultrasonic A-scan signal on the downhole portable monitor.

(a)

(b)

Figure 14. Uphole system. (a) Control van and communications cable; and (b) operator at the uphole system control console.

(a)

(b)

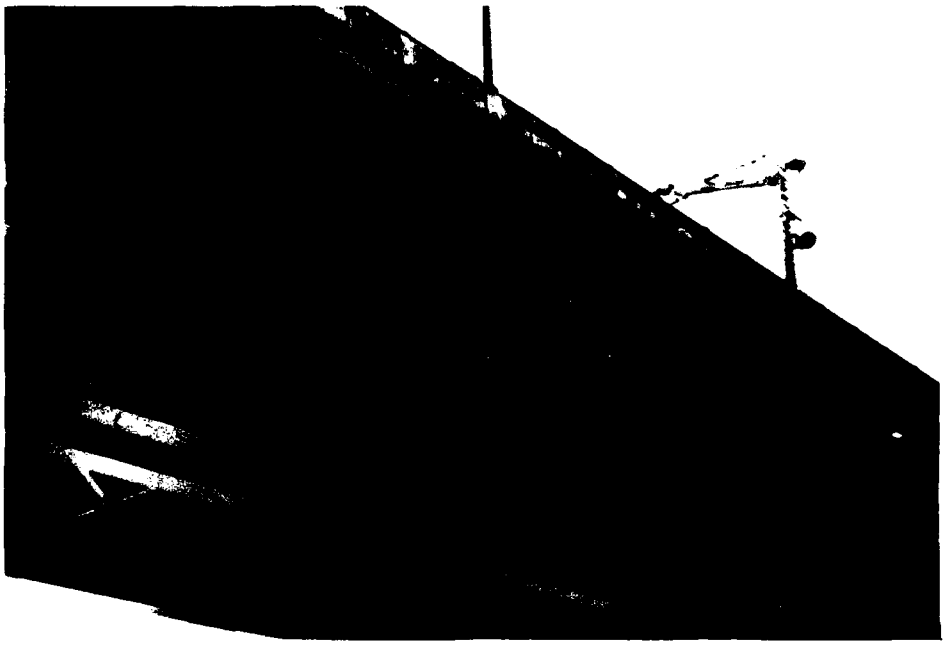

Figure 15. I-205 West Linn bridge. (a) Bridge; (b) snooper crane with inspection team.

(a)

(b)

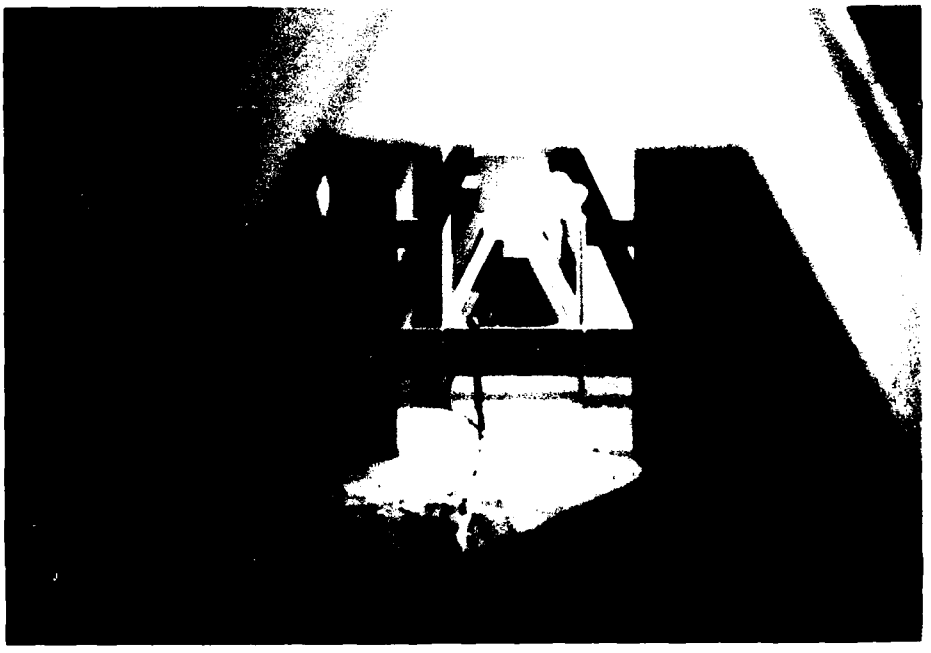

Figure 16. I-205 West Linn bridge. (a) Access to girders; (b) inside box girder.

(a)

(b)

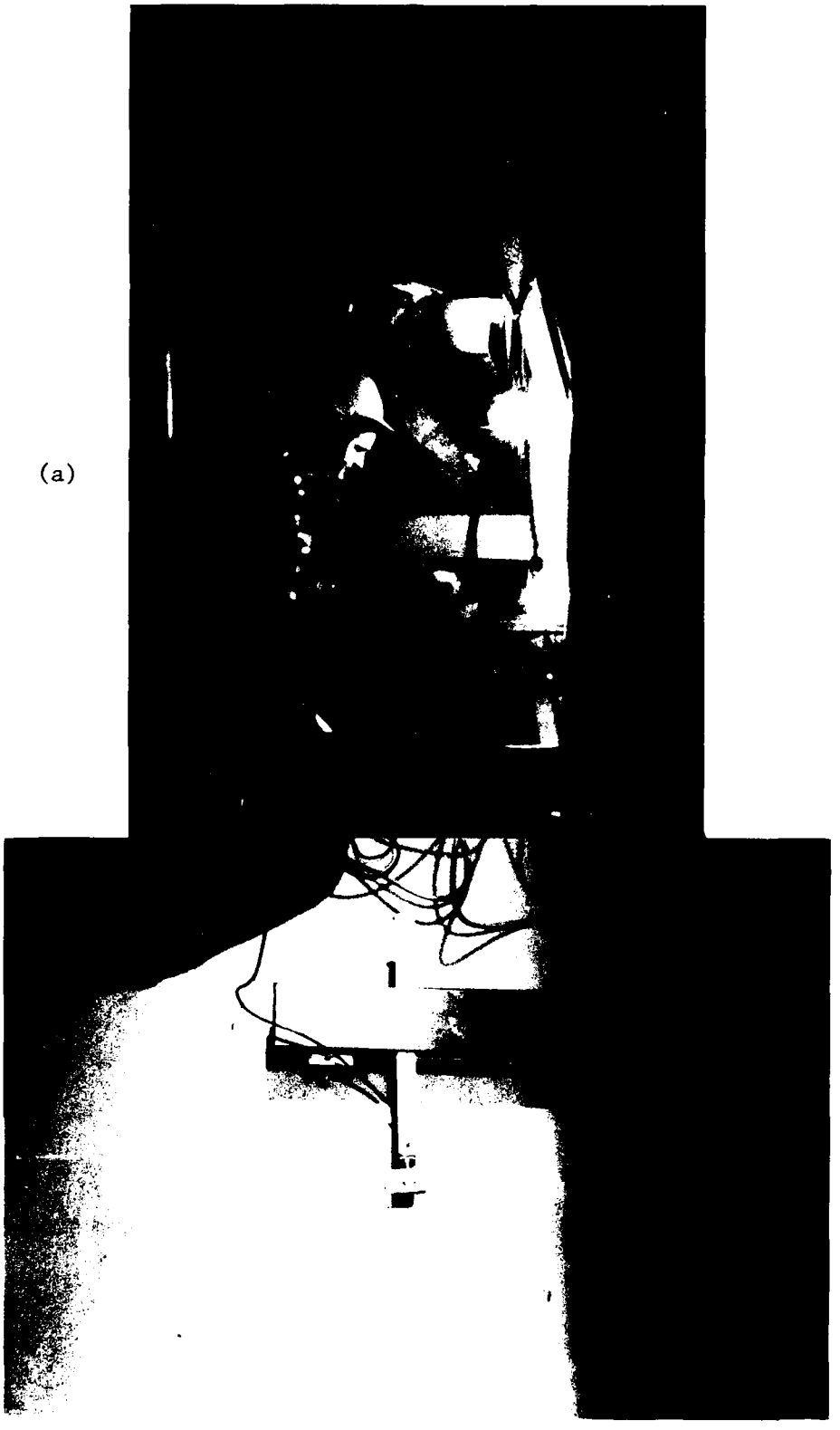

Figure 17. Inspection of West Linn Box girders. (a) Inspection team; (b) scanner over bottom flange weld.

Conclusions of Field Trials

The field trials resulted in several ideas on system improvement. It was found that the size of the scan aperture could be reduced and still be effective. The scanner arm was therefore reduced in size to a 7.5-inch aperture and this made field operations easier to perform because the originally designed 17-inch aperture arm could be a problem in close quarters inspection areas. The 7.5- by 11-inch scan aperture is sufficient to image most flaws of interest.

Field testing also showed that it is also necessary to use the A-scan method to detect flaws. Once a flaw is detected, if it appears to be significant, the automated imaging system is used to obtain an image of the defect. It is impractical to employ the scanning system on the entire structure. The cost-effectiveness of the labor and the massive amount of data that would have to be stored and analyzed preclude using the scanner to cover the entire structure. By using an adequate detection procedure to determine whether or not a localized area has indications needing documentation and analysis, the total amount of data stored is reduced by many orders of magnitude and the amount of time required to inspect the bridge is reduced by a large amount. The flaw image from the automated hand-scan image becomes a permanent record. In order for the inspector to know when to image a flaw a threshold response needs to be established. No universally accepted criteria exist today. The field trials indicate that a multilevel approach to inspection should be used. The first level is the relatively rapid A-scan flaw detection testing. The second level is the automated imaging of the flaw using the amplitude and TOF displays. The third level is the use of the holographic imaging and reconstruction. A second scan using an optimized transducer for the holographic data acquisition may be required in that case. The process of detecting the presence or absence of a defect in an arbitrary volume has different optimal transducer parameters than does the process of characterizing a defect that has been detected. The transducers used in the automated imaging system are a compromise between the two different processes. If the need is for the most accurate dimensions and characteristics of a defect that has been detected, then the transducer should be changed and the frequency, size, and focal pattern chosen to optimize the holographic process.

Even with the data improvements of the automated imaging system, hand-written records are important in the field. The location of the scanning must be noted and if possible painted on

the bridge structure for later repeat testing. The receiver attenuation setting, and gate settings must also be noted in a log book because the data information header in the computer does not record these values. The gate settings are very important because they determine the portion of the ultrasonic waveform that is used to create the image.

TEST RESULTS ON FLAWS

Phase II Results

The Phase II test specimens were listed in table 2. These samples represented materials and configurations of interest in bridge structure inspection and in some cases contained a number of flaws.

The Wisconsin Department of Transportation and the General Dynamics test blocks were used for ultrasonic beam testing. The Wisconsin DOT blocks contained electroslag welds that can be difficult to penetrate. They also had thickness transitions at the weld. The beam testing was to verify that the transducers and UT mainframe were capable of penetrating the electroslag weld zone with acceptable signal strength and with an acceptable level of background noise. Electroslag welding normally creates a relatively large grain size in the weld zone and the adjacent heat affected zone (HAZ). As the grain size increases in metals, the penetrating power of an ultrasonic beam decreases and the level of background noise increases. The combination of less penetrating power and more noise makes it more difficult to detect flaws and introduces more uncertainty into flaw analysis. The automated imaging system acoustic mainframe could satisfactorily see through the weld. The hand scanner could also be used on the thickness transition welds using angle beams. The hand scanner allows the arm to be tilted and the transducer mount allows the transducer to angulate on uneven surfaces. This combination makes the hand scanner acceptable for inspection over surface contour changes such as weld transition. Because these transitions will cause a change in the beam path length in the material, the inspector must consider this in the gating of the ultrasonic signal and interpretation of the image display.

The General Dynamics test plate was actually a specimen used for shipbuilding. The HY-80 material is used in marine structures rather than bridge structures. The testing on this block however showed that bounce path inspection using the automated imaging system ultrasonics system was acceptable for defect detection and imaging.

The Lehigh University blocks contained cracks at the cover plate to I-beam flange fillet welds. Figure 18 is a sketch of the sample configuration. Measurements on these cracks indicated that they were surface breaking cracks of typically 0.5 inch depth and

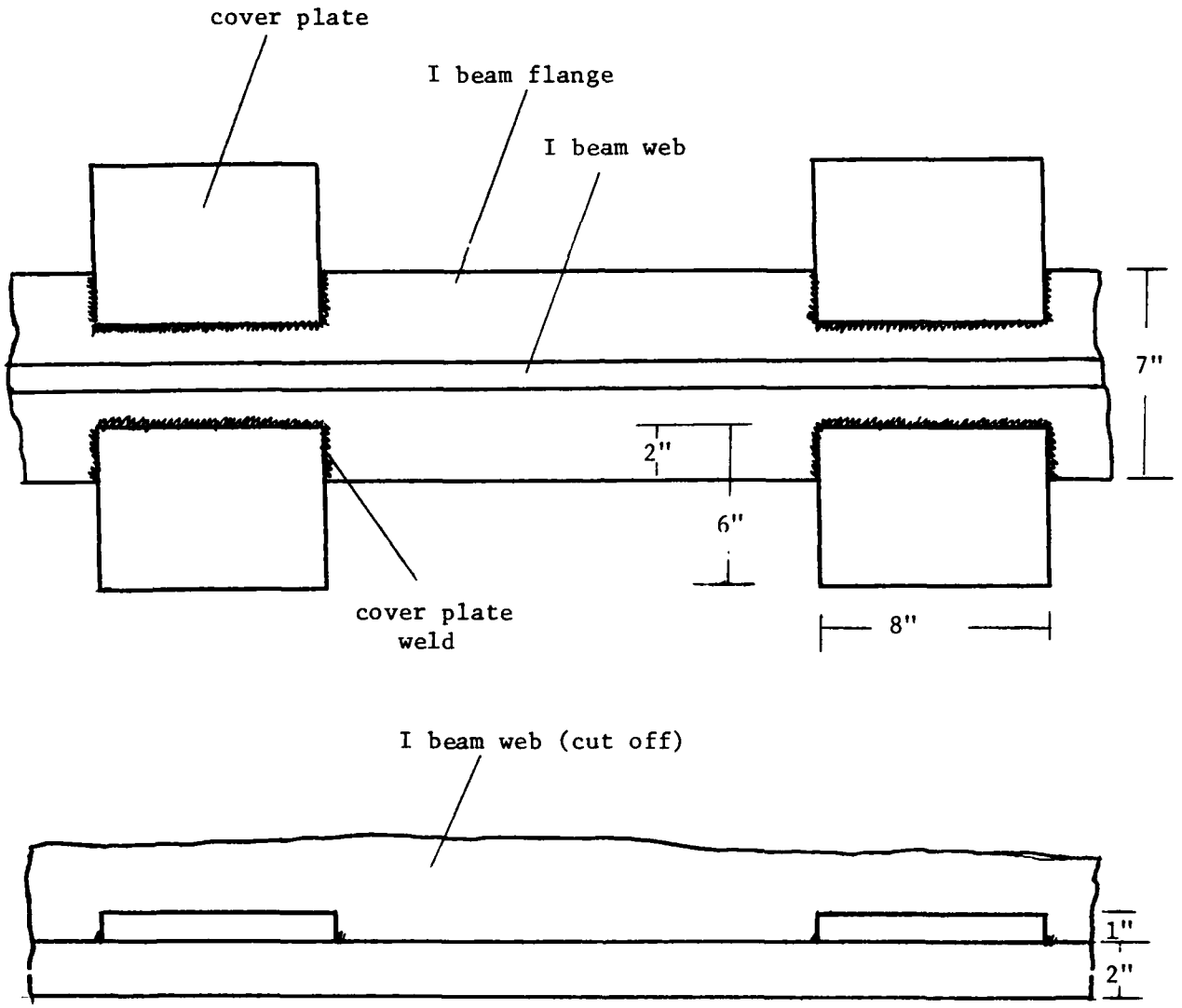

Figure 18. Sketch of Lehigh University test samples (not to scale).

1 inch and greater lengths. Figure 19 shows the imaging results on such a crack using the automated imaging system. The vertical axis in these images is the scan along the crack length. Figures 19a and 19b were obtained with a 5.2-inch by 5.1-inch scan using a 2-MHz transducer at 45 degrees. The images include a geometric reflector due to the fillet weld geometry in addition to the crack. Figure 19a is the amplitude C-scan. Figure 19b is the holography reconstructed image. In the holographic reconstruction the flaw and geometric reflector are separated (the flaw on the right and the geometric reflection on the left). Image sizing in the length dimension is 1.5 inches (3.86 cm) and 1.3 inches (3.35 cm) for the amplitude scan and holographic reconstruction respectively. The through wall extent of the crack estimated from the data is 0.6 inches. Figure 19c is a holographic reconstruction from a 1.4-by .4-inch scan using a 60 degree beam. The geometric reflector is not significant at this beam angle.

The four Oregon Graduate Center test samples were manufactured with numerous weld defects. The welding process was electroslag welding. This processed is believed to be a worst case grain structure for inspection that could be expected to be found on existing bridge structures. Figures 20 and 21 show the planned weld defect configuration. Table 3 lists the weld defect formations used. The numerous quantity of defects implanted actually inhibits inspection for a laboratory sizing study because of the proximity of neighboring defects to the defect under examination. Nevertheless images were obtained on test samples and correlated to x-rays of the samples. The defects of interest were crack-like defects. Angle beam measurements were used. Figure 22 shows the image of a crack like defect in test block DF-4. The scan was 7.68-by3.84-inches with a 2.25-MHz transducer at 45 degrees. The x axis is along the crack length. Figure 22a is the amplitude scan on the left with a zoom of the inset area shown on the right. The operator zooms an area by placing the cursor at the object he wishes to zoom. The cursor defines the center of the area that will be zoomed. The appropriate function key is pressed (F7 for pixel replication zoom or F8 for smooth zoom) and the zoom value is input. The operator inputs the zoom value from the keyboard, and the area in the plot that will be expanded to fill the zoom image is shown by the small box drawn about the cursor in the data plot. Figure 22b is the TOF profile. The vertical scale tic marks are 20 microseconds. The flaw is imaged in the center, large array of dots. The line below is the back of the gate. The TOF profile plot in figure 22b is a composite of the TOF data plotted as time (the vertical axis) versus distance in the x axis direction (the horizontal axis). Each tic-mark on

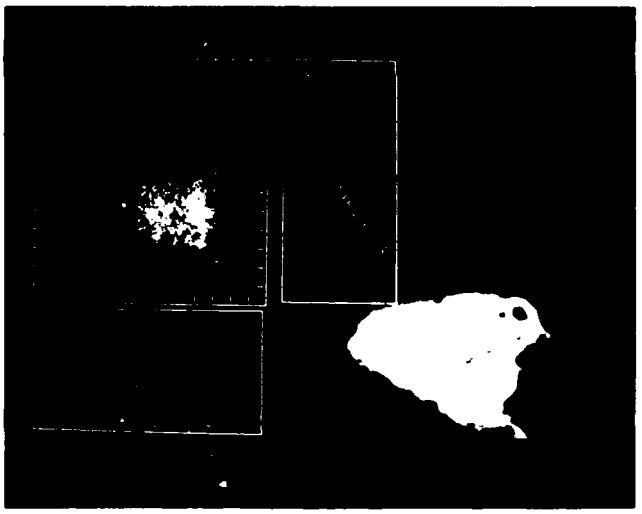

(a)

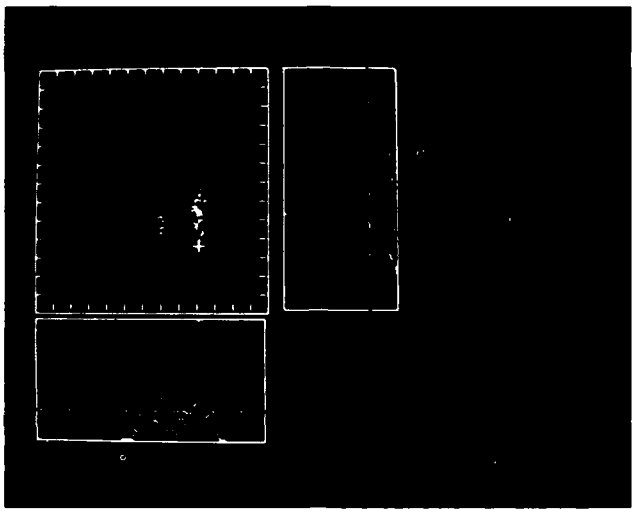

(b)

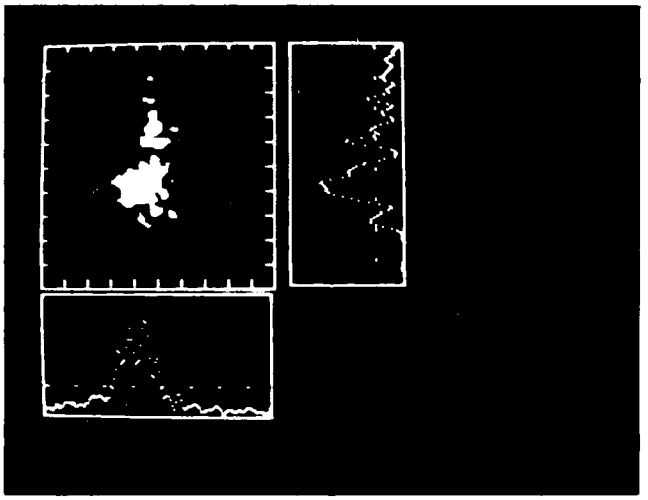

(c)

Figure 19. Images of a crack in the Lehigh University test block. (a) 45 degree beam amplitude C-scan; (b) 45 degree beam holographic reconstruction; (c) 60 degree holographic reconstruction. (Rectangular side boxes are x and y data profiles at the cursor location.)

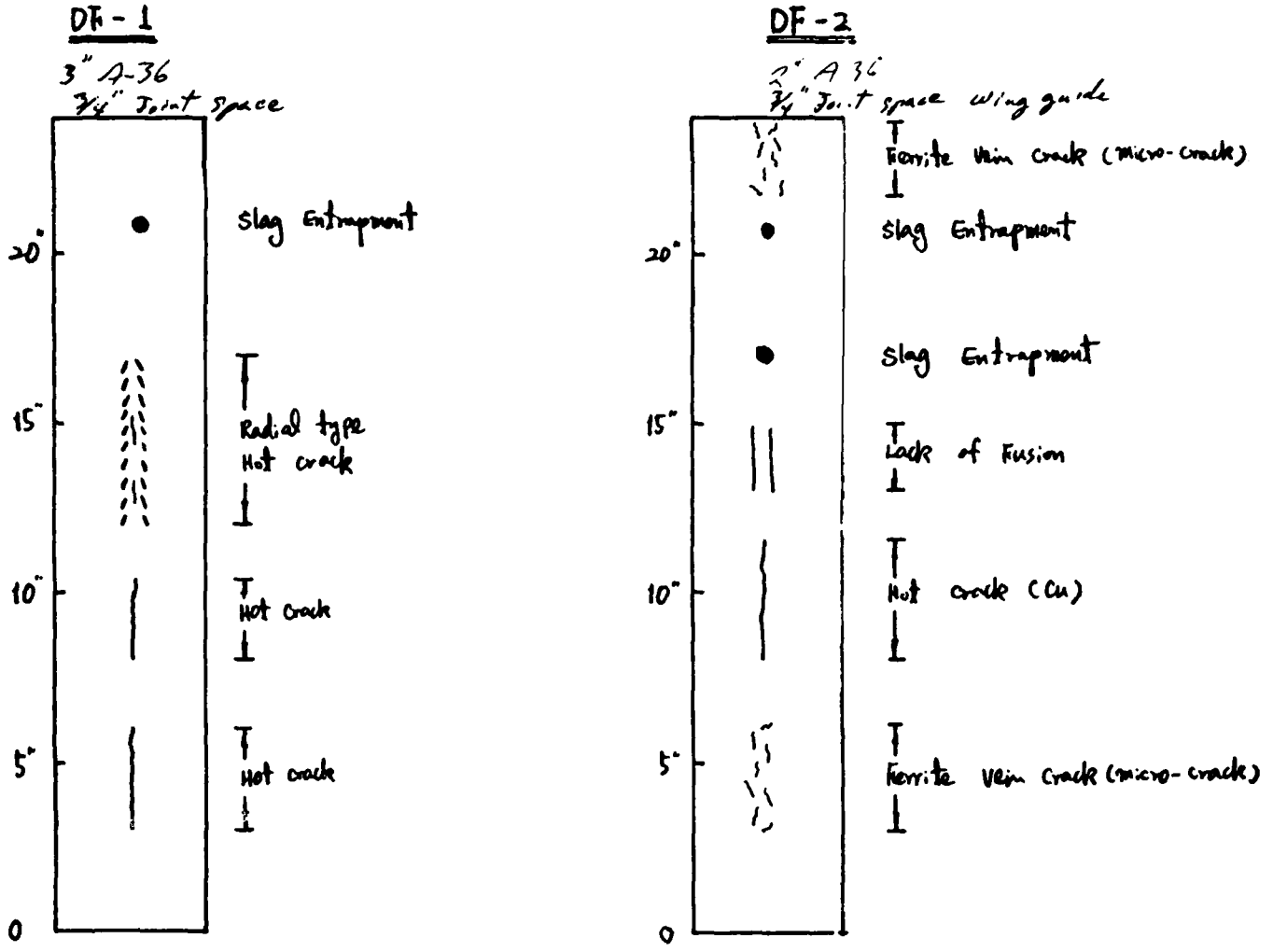

Figure 20. Planned weld-defect configuration in the Oregon Graduate Center test samples DF-1 and DF-2.

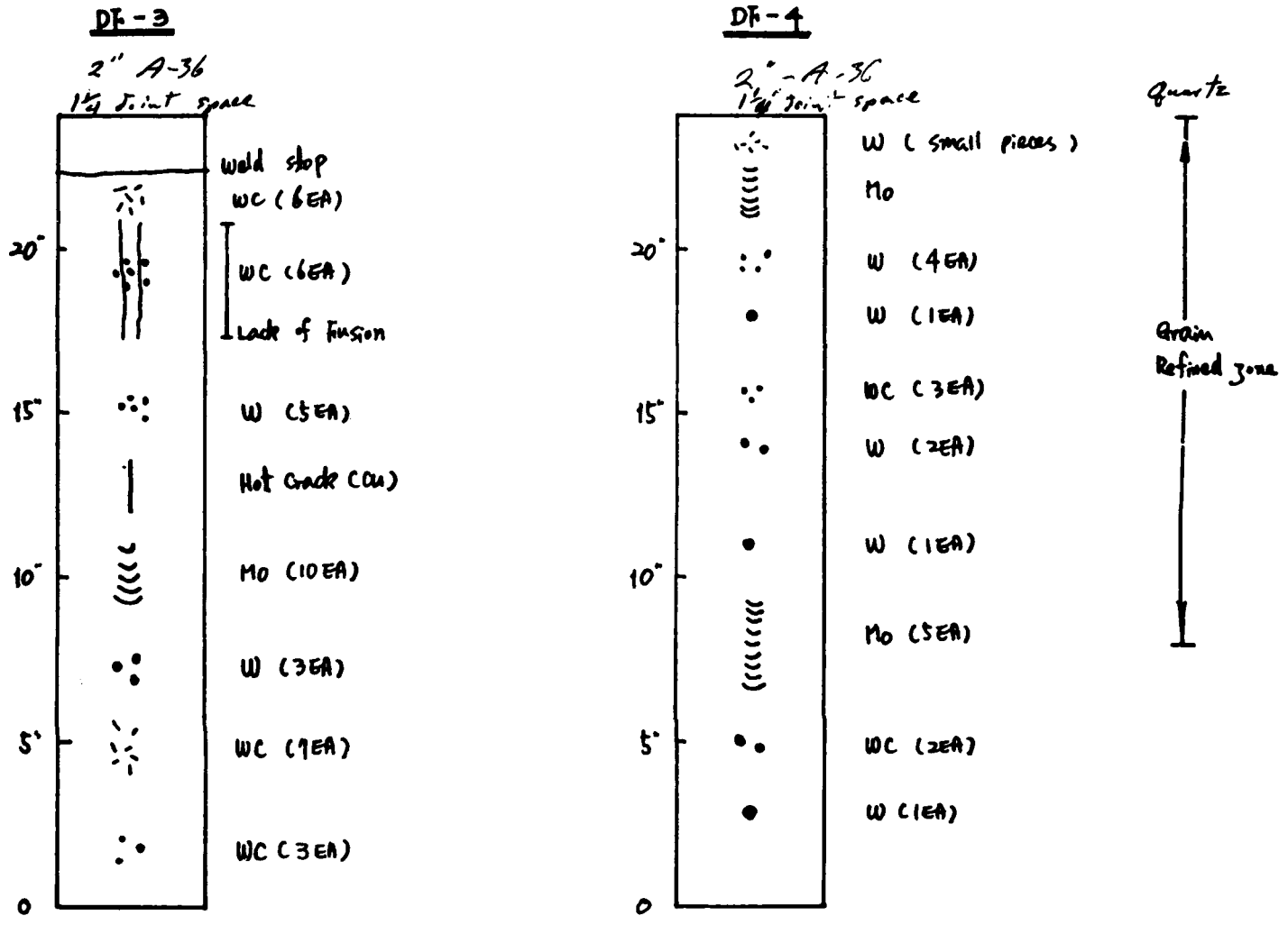

Figure 21. Planned weld-defect configuration in the Oregon Graduate Center test samples DF-3 and DF-4.

Table 3

Defect formation for Oregon Graduate Center test blocks

Defects	Welding Conditions	DF-1	DF-2	DF-3	DF-4
Lack of Fusion	Low Voltage (Low Heat Input)	x	x	x	x
Hot Crack					
*Centerline	High Current	x	x	x	
*Radial	Cu Addition	x	x	x	
Ferrite Vein Crack	Hydrogen Wet Flux CaO Addition		x		
Slag Entrapment	Weld Stop and Restart Low Voltage	x	x		
Inclusion	Elements Addition				
*Mo				x	x
*W				x	x
*WC				x	x

Summary:

UT: Difficult Inclusion Detection and Ferrite Vein Crack
RT: Difficult Ferrite Vein Crack
AH:

(a)

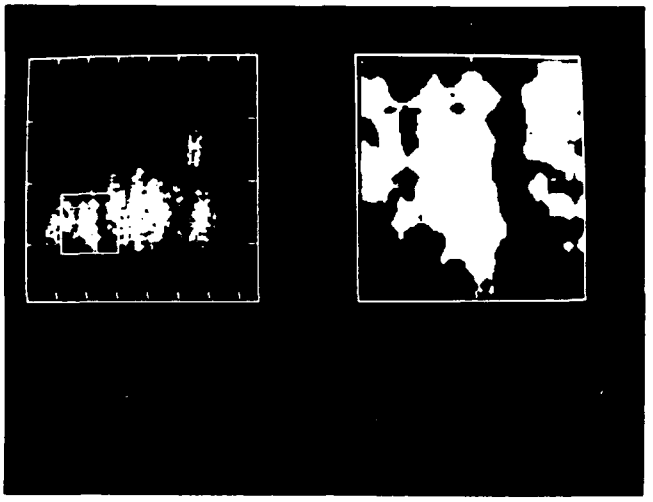

(b)

Figure 22. Defect in sample DF-4 from the Oregon Graduate Center. Data taken at 45 degrees, 2.25 MHz with a scan size of 7.7 by 3.8 inches. (a) Amplitude C-scan plot with zoomed image; (b) TOF profile (vertical scan units of 20 microseconds, flaw is imaged between 80 and 100 microseconds, the horizontal line at 125 microseconds is the back of the gate).

the horizontal axis equals one inch. A plot of this type is called a B-scan (XT plot) and represents and 'end view' looking through the material at a projection of the defect. The plot in figure 22b is the combination of all the 'slices' overlayed on the same plot to give the complete profile of the defect in the B-scan plot.

Figure 23 shows the amplitude C-scan images of three defects in block DF-1. Measurements of the defect lengths along the x axis are respectively 2.16, 1.52, and 1.88 inches for images 23a, 23b, and 23c. X-ray results indicated sizes of 2.0 and 1.5 inches for the a and b defects. The x-ray image indicated a compound flaw for defect c of length 1.5 to 2 inches. Figure 24 shows a TOF plot of defect c. By observing the vertical profiles (figure 24b contains more overlays in the vertical profile than figure 24a), the presence of multiple reflectors is detected. The compound nature of the flaw is indicated by the multiple slopes in the vertical TOF profiles. The different slopes shown in the profile windows on the right of the main plot window are the result of an angle beam inspection of defects that lie at different depths, or at different distances from the weld centerline. When an angle beam inspection is performed, the reflected signals from a defect do not remain at constant time value because the total distance between the transducer on the surface of the test area and the defect changes as the transducer is moved about. When multiple objects in a weld zone are present, it may not be possible to visually differentiate between them by looking at the A-scan or amplitude plots. The TOF profiles in this display are able to show the presence of different defects in the same area because the characteristic time change as a function of transducer position have different slopes as shown in the profile windows in figure 24a and 24b.

Figure 25 shows the results of imaging a defect in test block DF-2. The amplitude plot of figure 25a indicates a defect length of 2.0 inches using a 25 percent threshold on the display. The TOF profile of figure 25b indicates a maximum through wall dimension of 1.55 inches. This value is obtained by measuring the depth difference between TOF profiles of the defect. The maximum depth difference divided by the cosine of the beam angle and divided by two for the round trip indicates the through wall dimension.

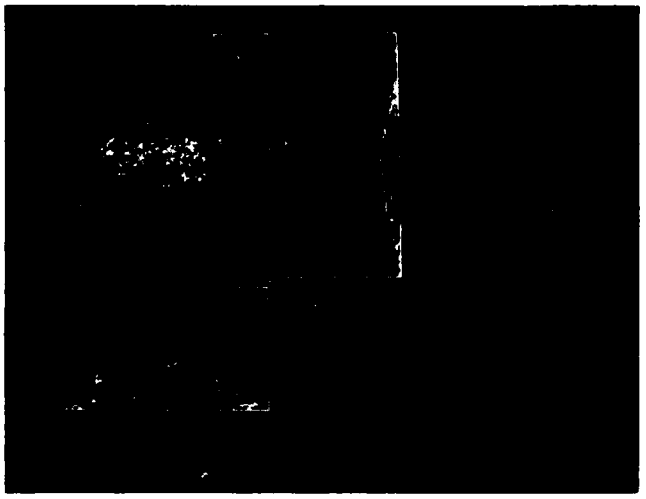

(a)

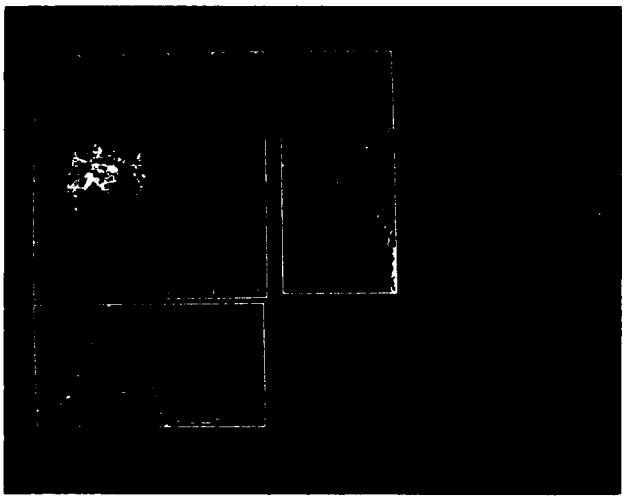

(b)

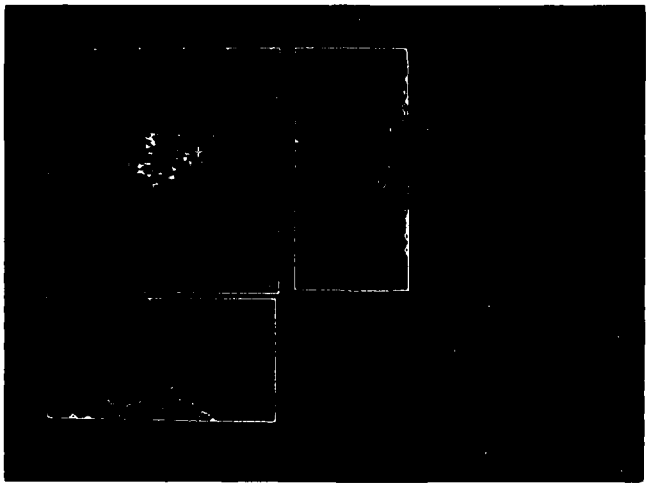

(c)

Figure 23. Amplitude C-scan plots of three defects in test block DF-1. (Images obtained using 45 degree beam, 2.25 MHz.)

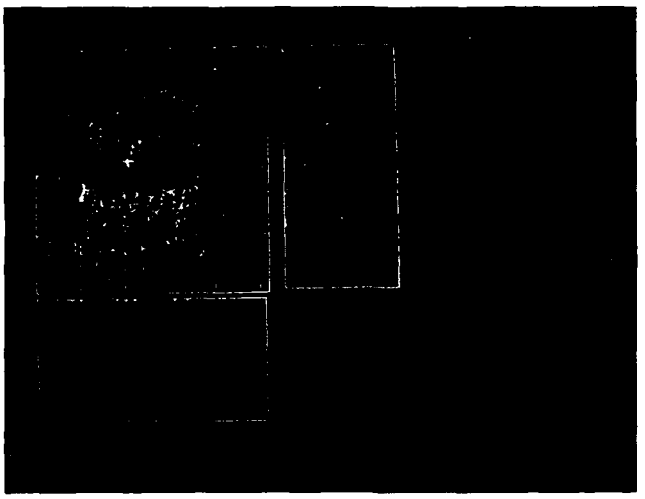

(a)

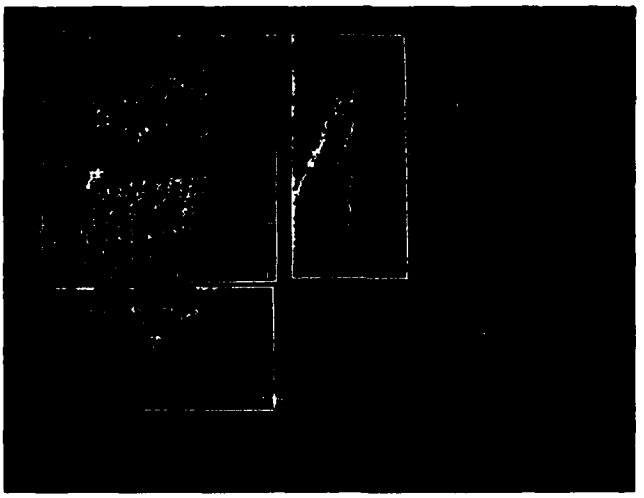

(b)

Figure 24. TOF images of the defect in figure 23c. These images are not interpolated and therefore show the hand scan coverage.

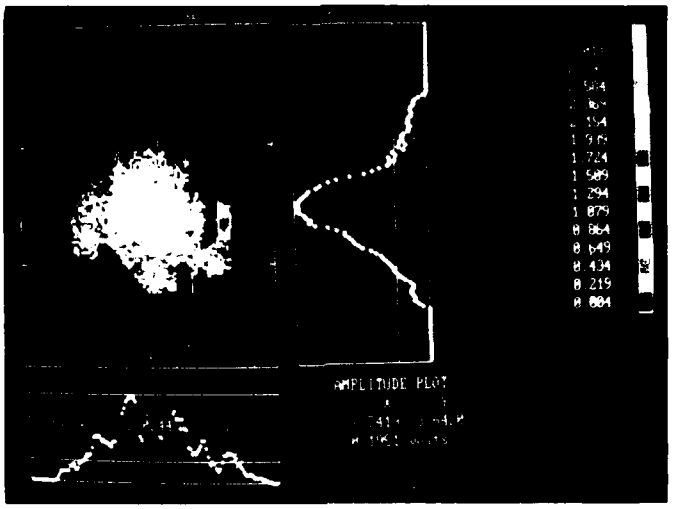

(a)

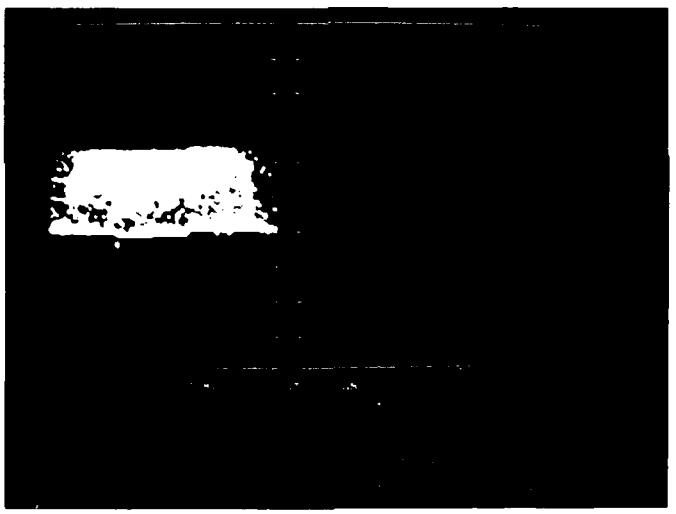

(b)

Figure 25. Defect in test sample DF-2. (a) Amplitude C-scan (3.2- by 2.9-inch scan aperture, 45 degree, 2.25 MHz); (b) TOF profile.

Destructive Test Comparisons

Destructive testing was performed on two of the Oregon Graduate Center test blocks of the Phase II laboratory samples. The destructive cuts in the block did locate the defects indicated by the ultrasonic tests. Unfortunately, the method of destruction was such that no through wall sizing information was available. Thus, no destructive sizing tests have been performed to correlate through wall dimensions with data taken by the automated imaging system.

Phase III Results

The Phase III inspections of the I-90 Mercer Island and I-205 West Linn bridges encountered defects only in the West Linn bridge. The defects of interest in the West Linn bridge were both delaminations and included defects (as opposed to surface-breaking) in the bottom flange welds of the box girders. Figure 26 shows the flange weld plan for the bridge. Figures 27 and 28 show the images of two inclusion defects in welds A1B4 and A3B1 respectively. The figure 27 image (A1B4 weld) shows a physically large defect. The scan aperture is 7.2 by 6.3 inches using a 45 degree, 2.25-MHz beam. Figure 28 uses the same angle beam on a 7- by 5.7-inch aperture scan. Figure 29 is map of a flange weld showing the location of four scan areas in box girder A weld A1B1. Figures 30 through 33 are image of delamination defects in the weld using a 5-MHz transducer in straight beam mode. In Figure 33b, the holographic data and a holographic reconstruction are shown. The reconstructed holographic image is thresholded to reduce noise. Figure 33 is holographic reconstruction of the A1B1-2 defect. Sizing estimates for some of the I-205 West Linn bridge images are in table 4.

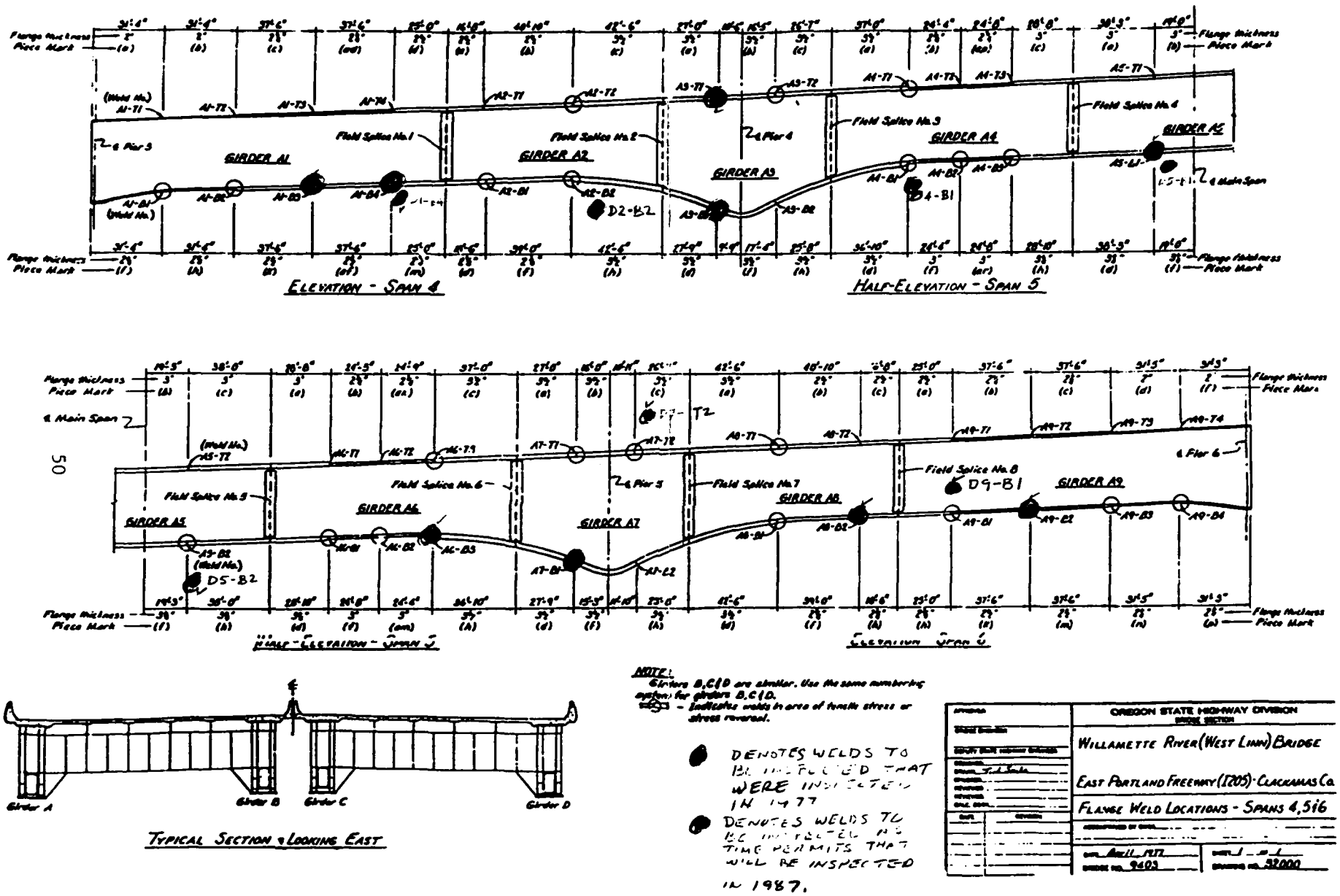

TYPICAL SECTION ℄ LOOKING EAST

NOTE:
Girders B,C&D are similar. Use the same numbering system for girders B,C&D.
- Indicates welds in area of tensile stress or stress reversal.

● DENOTES WELDS TO BE INSPECTED THAT WERE INSPECTED IN 1977

● DENOTES WELDS TO BE INSPECTED AS TIME PERMITS THAT WILL BE INSPECTED IN 1987.

OREGON STATE HIGHWAY DIVISION
BRIDGE SECTION

WILLAMETTE RIVER (WEST LINN) BRIDGE

EAST PORTLAND FREEWAY (I205) - CLACKAMAS Co.

FLANGE WELD LOCATIONS - SPANS 4,5&6

DATE April 1977 | SHEET 1 OF 1

DRAWING NO. 9403 | DRAWING NO. 32000

Figure 26. I-205 West Linn bridge flange weld locations.

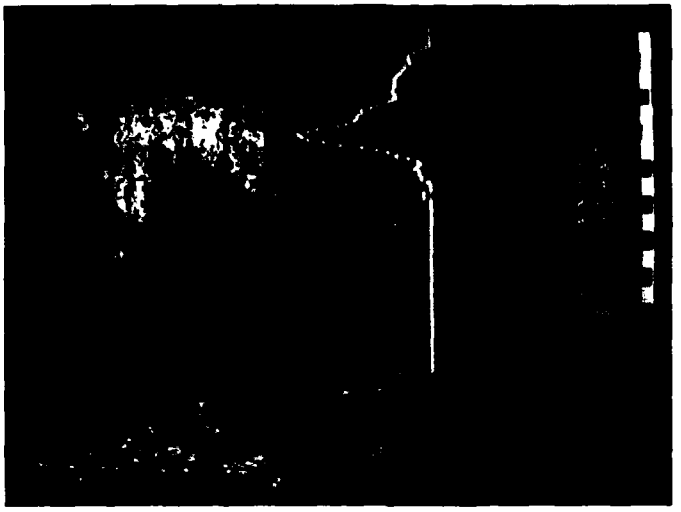

Figure 27. Image of a defect in flange weld A1B4 using a 45 degree, 2.25-MHz beam. Amplitude C-scan using a 25% threshold.

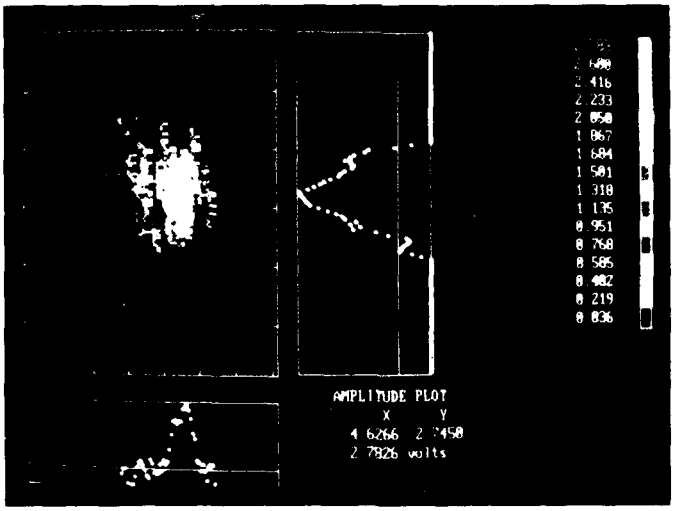

Figure 28. Image of a defect in a flange weld A3B1 using a 45 degree, 2.25-MHz beam. Amplitude C-scan using a 25% threshold.

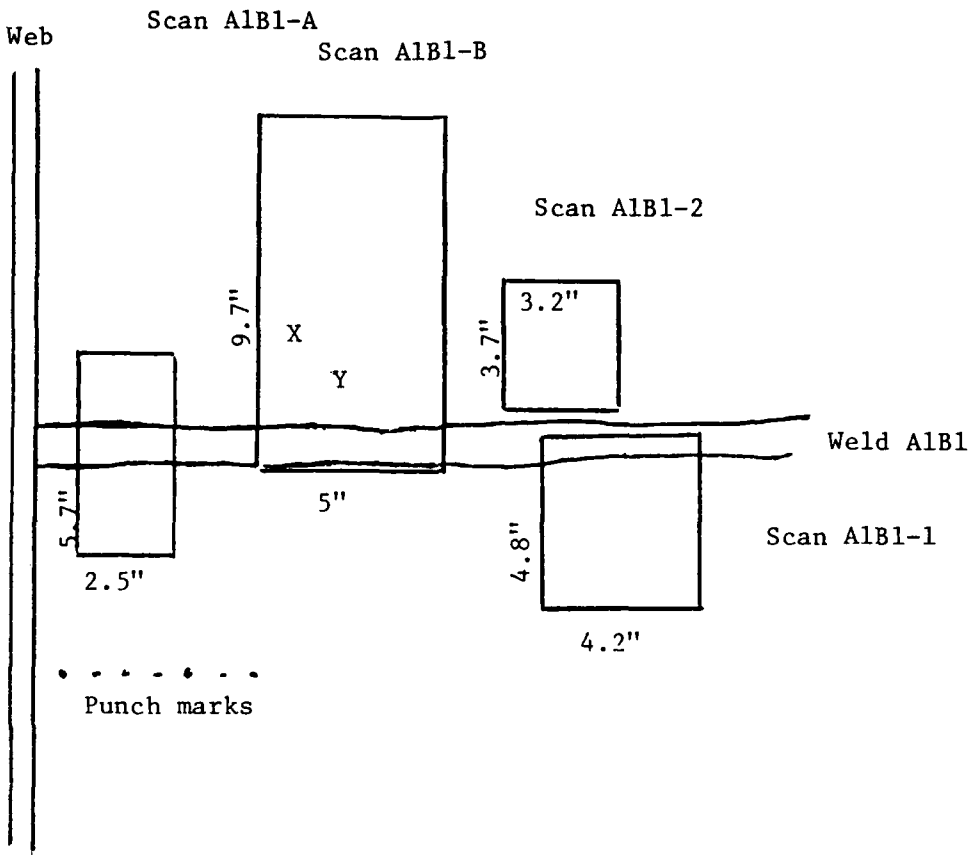

Figure 29. Map of approximate scan locations in box girder A-weld A1B1.

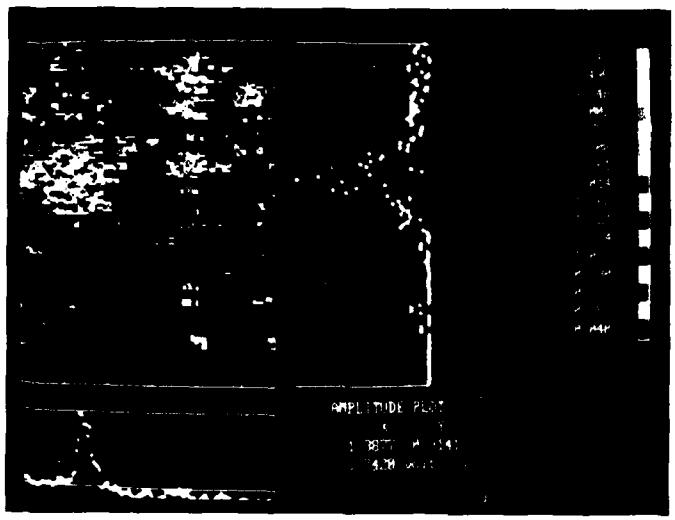

Figure 30. Image of defect A1B1-A. Amplitude C-scan using a 15% threshold. Scan aperture is 5.73 by 2.25 inches, 5 MHz, straight beam.

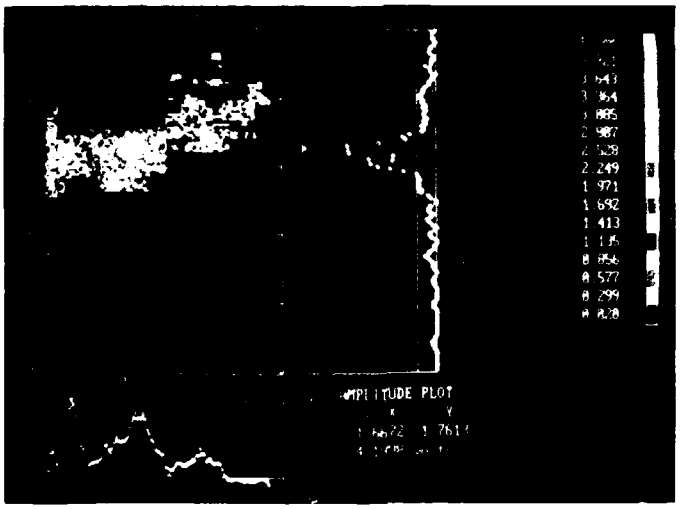

Figure 31. Image of defect A1B1-B. Amplitude C-scan using a 15% threshold. Scan aperture is 9.7 by 5.0 inches, 5 MHz, straight beam.

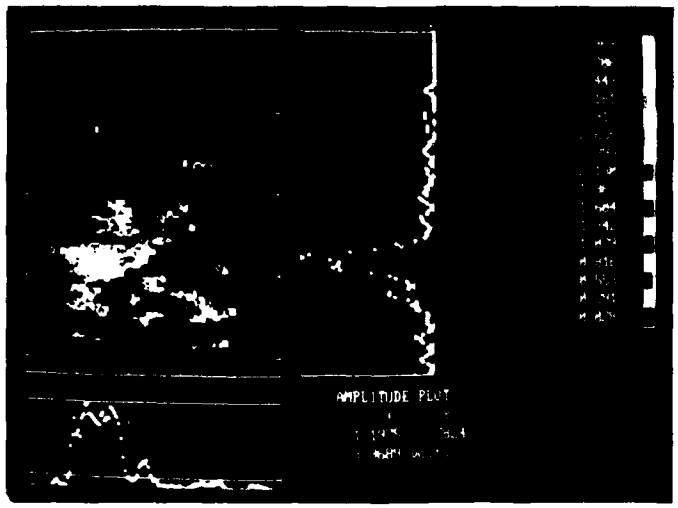

Figure 32. Image of defect A1B1-1. Amplitude C-scan using a 15% threshold. Scan aperture is 4.79 by 4.19 inches, 5 MHz, straight beam.

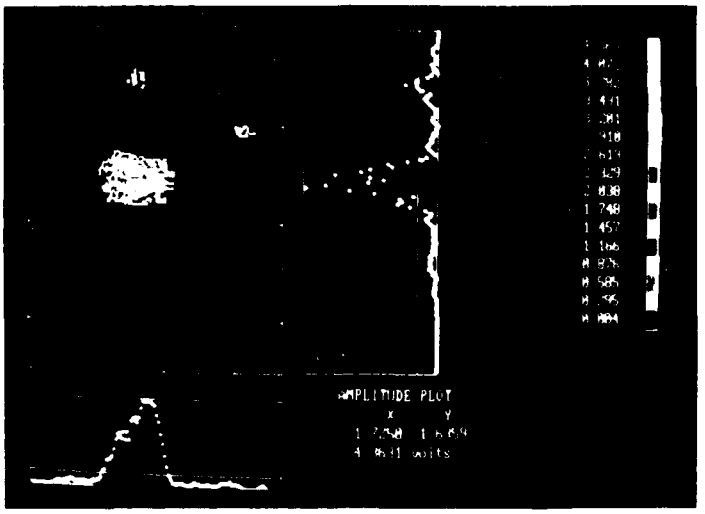

(a)

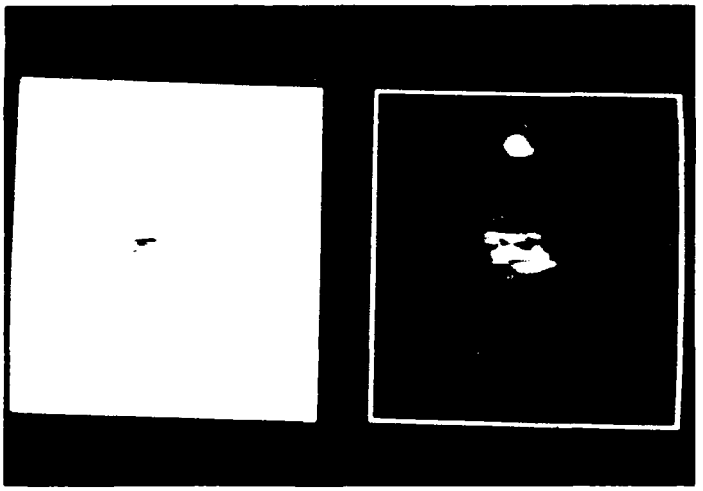

(b)

Figure 33. Image of defect A1B1-2. 5 MHz, straight beam with a scan aperture of 3.68 inches. (a) Amplitude C-scan plot at 15% threshold; (b) holographic result (left:cosine raw data, right: holographic reconstruction magnitude).

Table 4

West Linn bridge inspection results

Data File	Length	Width	TWD*	DBS**
A1B1-B	7.12	0.90	NA***	0.79
A1B1-A				
#1	1.16	0.40	NA	0.58
#2	0.80	0.31	NA	0.67
#3	0.45	0.12	NA	0.58
A1B1-1	1.12	0.39	NA	1.84
A1B1-2				
#1	0.95	0.46	NA	1.56
#2	0.32	0.16	NA	1.40
#3	0.17	0.10	NA	1.61
A3B1-2	0.51	NA	>0.05	3.45
A1B4-6	3.41	NA	0.17	NA
A3B1-3	0.61	NA	0.06	2.58
A1B4-5	0.50	NA	0.13	2.56

All dimensions are inches

*TWD: Through wall dimension
**DBS: Depth below the surface
***NA: Not available or not applicable

CONCLUSIONS

The automated imaging system for bridge inspection has been developed and demonstrated. The system is a workable, deployable compromise solution to the dual problem of detection and characterization operational needs. The equipment is state-of-the-art inspection technology and as such is finding interest in inspection needs other than bridge structures. The sophistication of the system for data acquisition and storage is not a burden to the operator. The sophistication of the data analysis is in the software and the operator is able to access this interpretation power through menus and function keys. The rugged design and packaging of the system is a significant achievement because most commercial systems with the accuracy and capability developed in this program are only available in the laboratory.

The usefulness of the automated imaging system has been demonstrated in field trials on bridge structures of interest. The system's imaging capability of flaws gives the inspector a much better understanding of the defect. The better understanding is a result of having the data displayed in ways that enhance the inspector's ability to determine flaw dimensions, flaw type and flaw location. The capability of post analysis and comparisons with previous or similar types of inspections also contribute to a better understanding of defects. The actual implementation of the system does not call for its use over the entire bridge structure. The inspector uses the traditional A-scan method to locate areas of flaws. If the flaw appears to be significant then the automated imaging system is used to obtain a permanent image record. This permanent record provides a repeatable standard for succeeding inspections of the structure. The system that has been developed provides an excellent base for repeat measurements. This is valuable for following the growth of flaws during the service life of the structure and for assisting in the determination of when repairs or replacements must be made.

The software developed in the program for data analysis is useful for defect characterization. Image-sizing measurements are made from the data using cursors. The amplitude and time-of-flight information is available to the inspector. The speed of the data processing is sufficient for some evaluation to be made while the inspector is on the bridge structure. The amplitude and TOF display is found to be useful for the majority of flaw characterization requirements. When angle-beam measurements are made the inspector must use care in interpreting the data to

account for the beam orientation in the structure and the transducer shoe time delay. Acoustic-holographic imaging is available in the system to provide the highest-resolution images if such precision is necessary.

It is expected that the automated imaging system for bridge inspection will become a useful tool for assuring highway safety.

RECOMMENDATIONS

This program has involved hardware and software development and field testing. A number of recommendations for the application and implementation of the system have been noted during the course of the project. Table 5 lists these recommendations. The recommendations fall into three categories: Application of nondestructive evaluation (NDE) to bridge structures, hardware improvements and software improvements.

The application of NDE to bridge structures needs to establish a more stringent criterion for the detection of flaws of significance. Once the criterion is established, the automated-imaging system can be applied as part of a routine inspection plan. The plan would call for the use of A-scan flaw detection by trained inspectors. When flaws are detected, the automated imaging system would be used to image those flaws. The locations of the scans would be permanently marked on the bridge structures and labeled in an appropriate manner in the data header. The images of the flaw would provide a permanent record of the flaw shape at a particular time. On-site amplitude and TOF analysis of the flaw would be sufficient in most cases to accurately evaluate the flaw size. The use of more detailed analysis could be performed away from the site using software routines including holography. Each State bridge authority should be encouraged to consider the utility of a field automated imaging system and should also obtain a compatible central-office computer and graphics display for post inspection analysis. This second computer, graphics, and software system would allow review and analysis of data at the central office while inspections are performed at field locations.

Hardware improvements to the system could be a valuable modification for future automated-imaging systems. Primarily these involve the computer hardware that has advanced even during the course of this program. Two areas of interest are higher speed and better data archival. Higher speeds will be available with newer computers and the use of faster processor boards such as array processors. Data archival will be a concern in the future as more and more data is obtained. Larger disk storage media and laser discs are worth considering. Provisions for other types of ultrasonic test equipment, ranging from conventional flaw detectors to more sophisticated methods should be addressed. Since the computer and scanner act as recording devices it is possible to substitute other inspection instrumentation that may

Table 5

Recommendations for the automated imaging system for bridge inspection

Application:

- Establish criteria for defect detections based on A-scan response.
- Use the automated imaging system to image detected defects.
- Maintain records of defect images using the bridge inspection system as the record keeper.
- Repeat measurements periodically to follow potential flaw growth.

Hardware Improvements:

- Update system with faster processors as equipment becomes available.
- Upgrade data storage to larger storage media.

Software Improvements:

- Update software following on operator experience with system to remove bugs and add features that operators desire.
- Improve image processing algorithms for faster processing.

be more appropriate to specific needs. The hardware and software should be configured for multiple types of data acquisition to take fuller advantage of the record keeping aspect of the system.

Software improvements to the system will always be of interest for updating the present software and implementing new schemes such as faster hardware and different storage media. Some algorithms within the current system structure may benefit from updating as greater field data is available. Also, operator preferences in the image and information display may be satisfied by changes to current algorithms. The development of algorithms to assist in the interpretation of angle beam measurements is an example. Use of the system by inspectors concerned with bridge structure defects will indicate what types of software improvements are desired.

The most important recommendation however is that the system be used by inspectors in the field. Their feedback will be useful in assuring that this system is in fact satisfying the national interest in ensuring the safety of highway bridge structures.

APPENDIX A
WORK BREAKDOWN STRUCTURE

AUTOMATED IMAGING SYSTEM FOR BRIDGE INSPECTION
WORK BREAKDOWN STRUCTURE

PHASE I

- Task A - Literature Survey
- Task B - Literature Evaluation
- Task C - Technique Evaluation

PHASE II

- Task A - System Assembly
  - A1 System Definition
  - A2 System Design
  - A3 Parts Procurement
  - A4 Algorithm Development
  - A5 System Simulation
  - A6 Mechanical Design
  - A7 System Assembly
  - A8 System Debug
- Task B - Test Block Design and Fab
  - B1 Design Weld Specimens
  - B2 Procure Weld Specimens
  - B3 Locate Base Metal Specimens
  - B4 Procure Base Metal Specimens
- Task C - Laboratory Testing

PHASE III

- Task A - Field Test
  - A1 Planning
  - A2 Bridge Selection
  - A3 Performance
- Task B - Analysis
- Task C - Modifications
- Task D - Demonstration
  - D1 Bridge Selection
  - D2 Performance
- Task E - Documentation
- Task F - Presentation

APPENDIX B
ADDITIONAL COMPONENT BLOCK DRAWINGS

Figure 34--Signal processor module block diagram.

Figure 35--Console junction box block diagram.

Figure 36--IBM AT card slot assignment diagram.

Figure 37--Belt pack block diagram.

Figure 38--Hand scanner controller board block diagram.

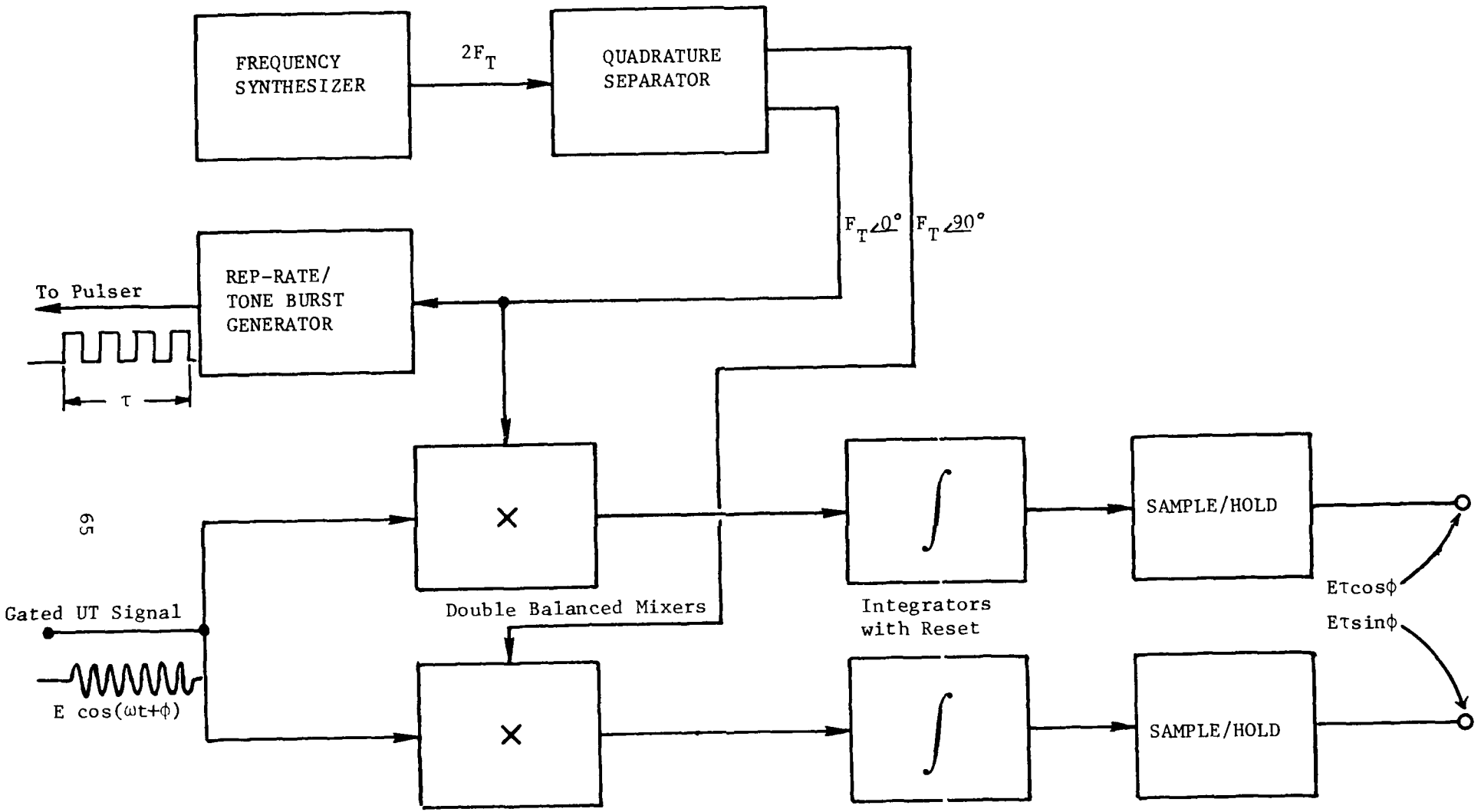

Figure 34. Signal processor module block diagram.

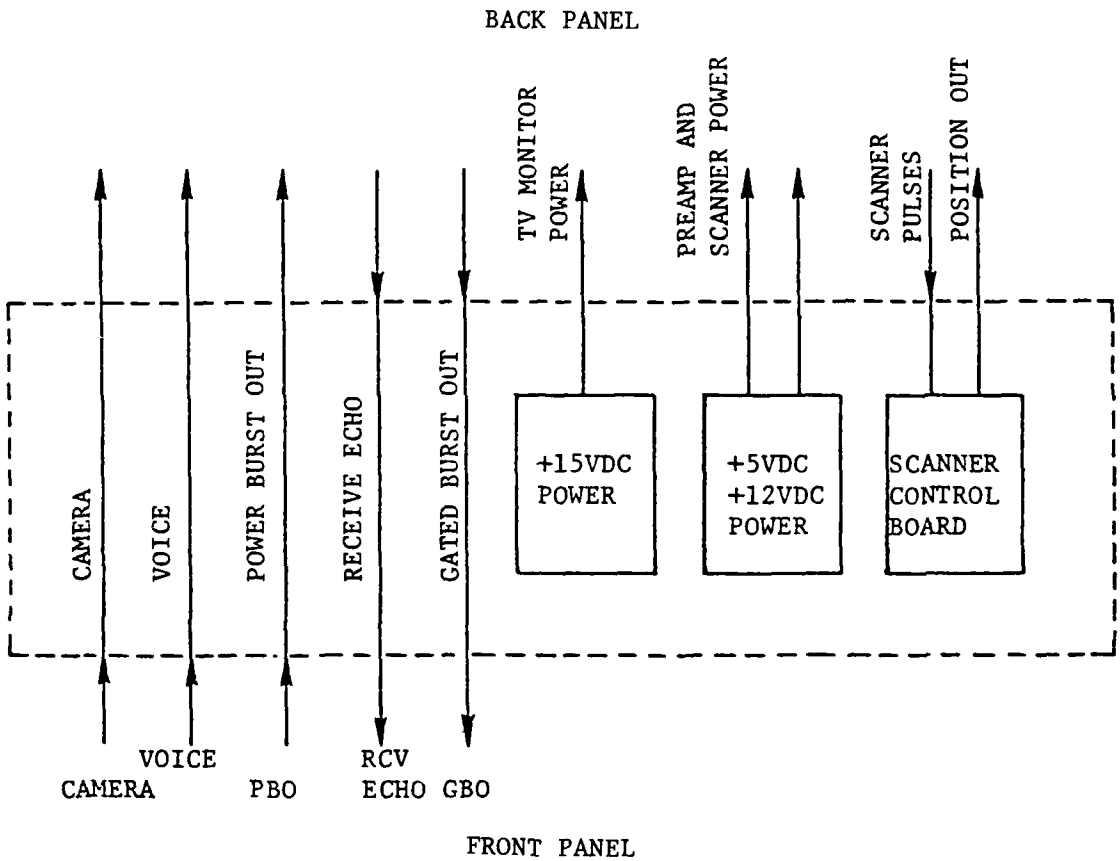

Figure 35. Console junction box block diagram. (All back panel connections go to the communication bundle except the "gated burst" which comes from the signal processor module and the "scanner position out" which goes to the IBM AT serial port.)

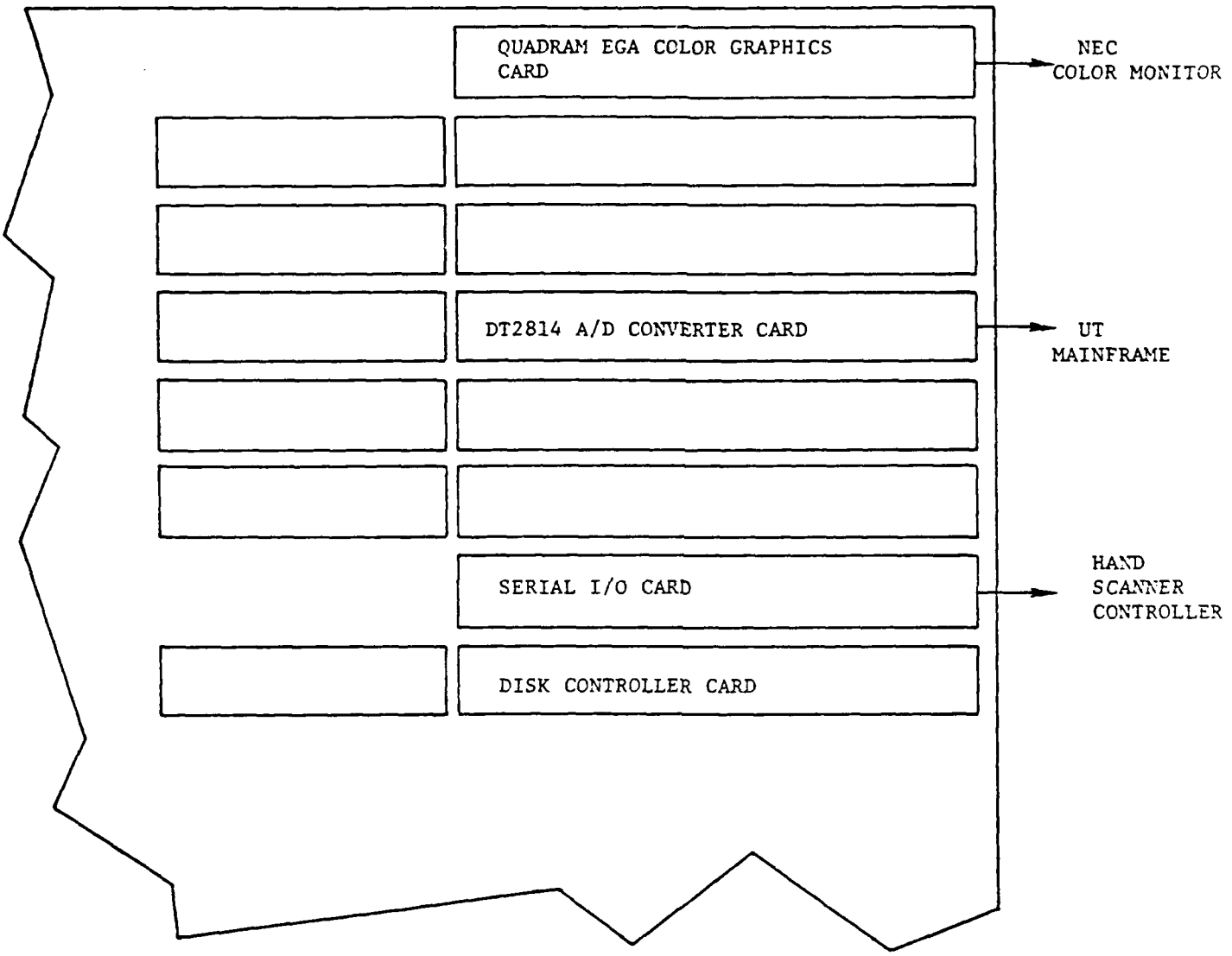

Figure 36. IBM AT card slot assignment diagram.

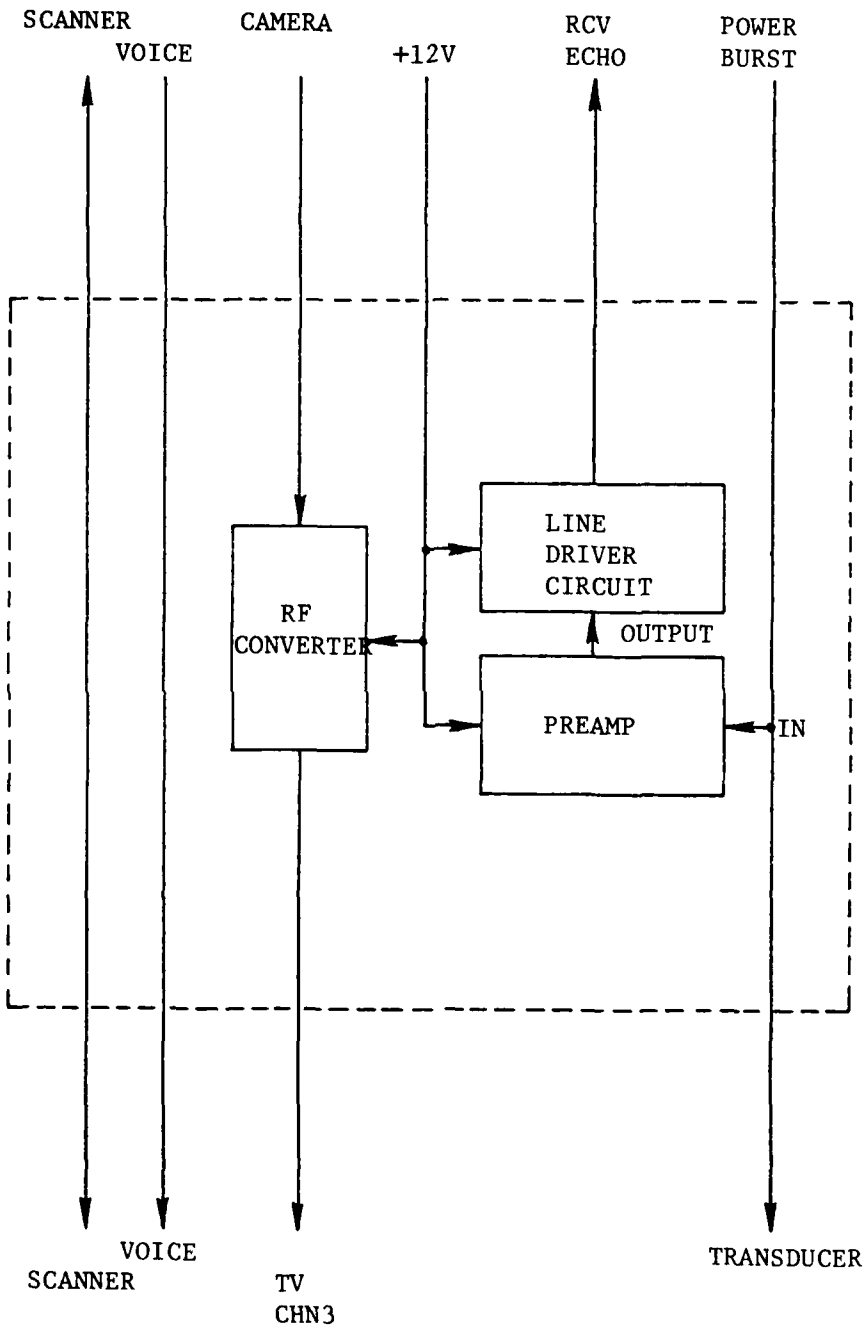

Figure 37. Belt pack block diagram.

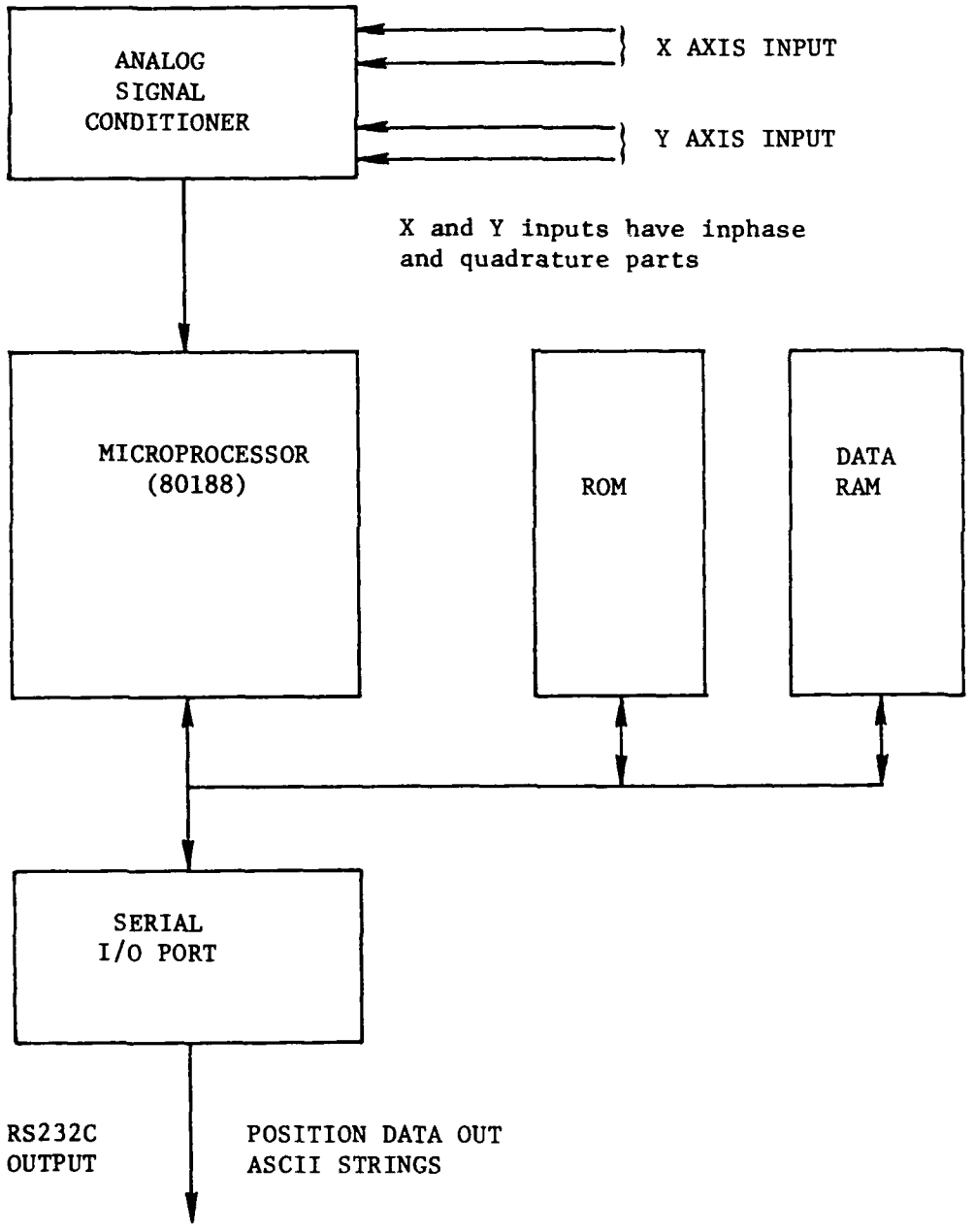

Figure 38. Hand scanner control board block diagram.

☆ U. S. GOVERNMENT PRINTING OFFICE: 1988--202-862--60090